# Supporting Information:

## Profiling Esterases in *Mycobacterium tuberculosis* using Far-Red Fluorogenic Substrates

Katie R. Tallman, Samantha R. Levine, and Kimberly E. Beatty

## Contents

## Materials and Methods

ACS grade solvents were used as received. DDAO was purchased from Shanghai Medicilon Inc. All other chemicals were purchased from Sigma-Aldrich, Fisher Scientific, or VWR Scientific and used as received. Unless otherwise stated, reactions were magnetically stirred. Reactions were monitored by thin-layer chromatography (TLC) on glass-backed silica gel plates (Silicycle 60 Å, 250 μM). Flash column chromatography was performed with the indicated solvents on Silicycle SiliaFlash P60.

Mass spectra were acquired at Portland State University's BioAnalytical Mass Spectrometry Facility on a ThermoElectron LTQ-Orbitrap Discovery high-resolution mass spectrometer with electrospray ionization (ESI).

NMR spectra were acquired at ambient temperature at Portland State University's NMR facility. $^{1}$H-NMR data were obtained in the specified solvent on a Bruker Avance II at 400 MHz. $^{13}$C-NMR data were obtained on the same instrument in the specified solvent at 101 MHz. Spectra were calibrated to the residual solvent peak. Chemical shifts are reported in ppm. Coupling constants (*J*) are reported in Hertz (Hz) and rounded to the nearest 0.1 Hz. Multiplicities are defined as: s = singlet, d = doublet, dd = doublet of doublets, t = triplet, m = multiplet, br s = broad singlet.

### Synthesis of iodomethyl butyrate

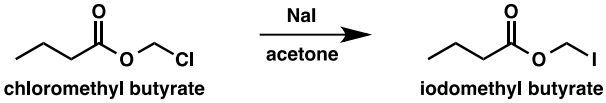


Sodium iodide (0.28 g, 1.97 mmol, 6 equiv) was combined with acetone (2 mL) in a 20 mL scintillation vial. Chloromethyl butyrate (0.25 mL, 1.97 mmol, 6 equiv) was dissolved in acetone (0.5 mL), and the solution was added to the vial dropwise via syringe. The syringe was rinsed with 0.5 mL acetone, and the vial was sealed and protected from light. After stirring overnight, 3 mL of $CH_2Cl_2$ was added to the vial, and the resulting mixture was filtered through fiberglass filter paper (Whatman GF/A). Concentration *in vacuo* and resuspension in $CH_2Cl_2$ was followed by a second filtration. Concentration of the resulting clear solution produced 0.277 g of iodomethyl butyrate as a brown oil (62% yield), which was used without further purification.

### Synthesis of DDAO-2-butanoylmethyl ether (DDAO-2-BME) and DDAO-7-butanoylmethyl ether (DDAO-7-BME)

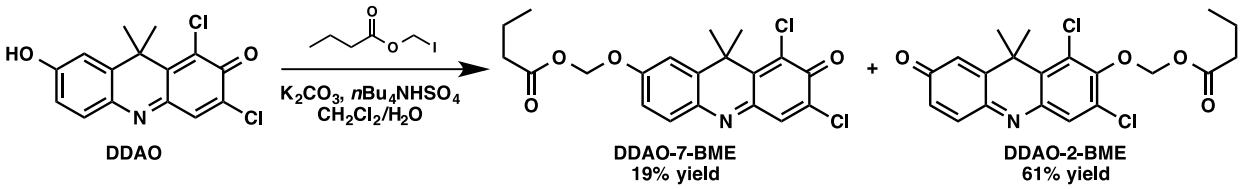


A 20 mL scintillation vial was charged with DDAO (0.1002 g, 0.325 mmol, 1 equiv) and tetrabutylammonium hydrogen sulfate (0.0112 g, 0.033 mmol, 0.1 equiv). Then $CH_2Cl_2$ (3.3 mL) was added, resulting in a deep red suspension. A solution of $K_2CO_3$ (0.1348 g, 0.975 mmol, 3 equiv) in $H_2O$ (1 mL) was added via pipet, followed by an additional 0.625 mL $H_2O$ (0.2 M total). The reaction mixture became dark blue upon vigorous stirring. Iodomethyl butyrate was added via pipet, followed by additional $CH_2Cl_2$ (1 mL, 0.08 M total), and the vial was sealed and protected from light. Additional $H_2O$ (2 mL, 0.13 M) was added after 21 h, and the reaction mixture was stirred for another 3 days. The reaction mixture was transferred to a separatory funnel with additional $CH_2Cl_2$ and $H_2O$. The layers were separated, and the organic layer was washed with $H_2O$ (1 × 15 mL). The combined aqueous layers were extracted with $CH_2Cl_2$ (3 × 15 mL). The combined organic layers were washed

with brine (1 × 20 mL), dried over $MgSO_4$, filtered, and concentrated *in vacuo* to a yellow-brown oil. Purification by column chromatography ($SiO_2$, loaded in toluene, 1.5 to 5% EtOAc in hexanes with 40% $CH_2Cl_2$ as a co-solvent) yielded two major products: an orange solid identified as DDAO-7-BME ($R_f$ = 0.66, 10% EtOAc/45% hexanes/45% $CH_2Cl_2$) (0.0248 g, 19% yield) and a yellow-orange solid identified as DDAO-2-BME ($R_f$ = 0.48, 10% EtOAc/45% hexanes/45% $CH_2Cl_2$) (0.0806 g, 61% yield).

**DDAO-2-BME (Figures S7-S10):**
$^1$H-NMR (400 MHz; $CDCl_3$): δ 7.74 (s, 1H), 7.35 (d, *J* = 10.1 Hz, 1H), 6.66 (d, *J* = 1.8 Hz, 1H), 6.66 (dd, *J* = 10.0, 2.0 Hz, 1H), 5.79 (s, 2H), 2.36 (t, *J* = 7.4 Hz, 2H), 1.78 (s, 6H), 1.65 (sextet, *J* = 7.4 Hz, 2H), 0.94 (t, *J* = 7.4 Hz, 3H).

$^{13}$C-NMR (101 MHz, $CDCl_3$): δ 187.36, 172.66, 153.08, 151.87, 148.30, 141.03, 140.59, 133.40, 132.68, 132.38, 129.62, 128.92, 127.97, 88.12, 38.17, 35.97, 28.91, 18.02, 13.77.

ESI-HRMS $[M+H]^+$ m/z calculated for $C_{20}H_{20}Cl_2NO_4$: 408.0764; found: 408.0774.

**DDAO-7-BME (Figures S11-S14):**
$^1$H-NMR (400 MHz; $CDCl_3$): δ 7.62 (s, 1H), 7.62 (d, *J* = 8.7 Hz, 1H), 7.13 (d, *J* = 2.6 Hz, 1H), 7.05 (dd, *J* = 8.7, 2.7 Hz, 1H), 5.85 (s, 2H), 2.37 (t, *J* = 7.4 Hz, 2H), 1.87 (s, 6H), 1.67 (sextet, *J* = 7.4 Hz, 2H), 0.94 (t, *J* = 7.4 Hz, 3H).

$^{13}$C-NMR (101 MHz, $CDCl_3$): δ 173.30, 172.43, 159.84, 148.54, 140.59, 140.57, 139.55, 137.12, 136.88, 135.08, 133.98, 114.86, 114.76, 84.52, 39.27, 36.10, 26.85, 18.30, 13.69.

ESI-HRMS $[M+H]^+$ m/z calculated for $C_{20}H_{20}Cl_2NO_4$: 408.0764; found: 408.0771.

**Synthesis of chloromethyl octanoate**

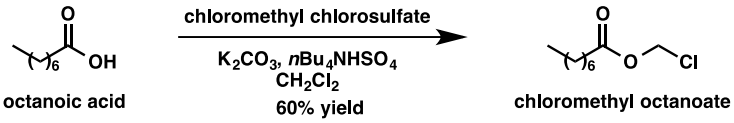


Octanoic acid (0.5 mL, 3.16 mmol, 1 equiv) and tetrabutylammonium hydrogen sulfate (0.0536 g, 0.16 mmol, 0.05 equiv) were dissolved in $CH_2Cl_2$ (3 mL) in a 20 mL scintillation vial. A solution of $K_2CO_3$ (1.75 g, 12.6 mmol, 4 equiv) in $H_2O$ (3 mL, 1 M final concentration) was then added, and the reaction mixture was stirred for 3 min. Chloromethyl chlorosulfate (0.4 mL, 3.94 mmol, 1.25 equiv) was dissolved in 3 mL $CH_2Cl_2$ (0.5 M total) and added to the reaction mixture portion-wise over 50 min. The reaction mixture was then stirred for an additional 70 min. The reaction mixture was transferred to a separatory funnel with additional $CH_2Cl_2$ and $H_2O$. The layers were separated, and the organic layer was washed with $H_2O$ (1 × 15 mL). The combined aqueous layers were then extracted with $CH_2Cl_2$ (2 × 15 mL). The combined organic layers were washed with brine and dried over $Mg_2SO_4$. Filtration and concentration *in vacuo* gave the crude product. Purification by $SiO_2$ plug (loaded in hexanes, 1 to 2.5% EtOAc in hexanes) and concentration *in vacuo* gave 0.36 g (60% yield) of the product as a clear, pale yellow oil. Spectral data matched that reported in the literature.[1]

**Synthesis of iodomethyl octanoate**

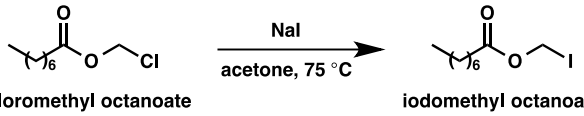


Sodium iodide (0.2548 g, 1.7 mmol, 1.01 equiv) was combined with acetone (2 mL) in a 2-dram vial. Chloromethyl octanoate (0.3221 g, 1.68 mmol, 1 equiv) in acetone (1 mL) was added dropwise,

followed by 1 mL acetone (0.42 M total). The vial was sealed and protected from light, and the reaction mixture was stirred for 7 h. $CH_2Cl_2$ (1 mL) was added, followed by filtration through fiberglass filter paper, concentration *in vacuo*, refiltration, and concentration under a stream of air to give an orange oil, which was used without further purification.

**Synthesis of DDAO-2-octanoylmethyl ether (DDAO-2-OME) and DDAO-7-octanoylmethyl ether (DDAO-7-OME)**

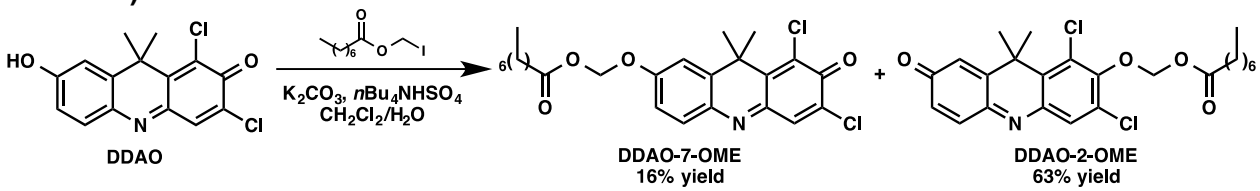


In a 20 mL scintillation vial, DDAO (0.1022 g, 0.332 mmol, 1 equiv) and tetrabutylammonium hydrogen sulfate (0.0113 g, 0.032 mmol, 0.1 equiv) were combined in $CH_2Cl_2$ (3 mL) to give a deep red suspension. A solution of $K_2CO_3$ (0.1376 g, 1 mmol, 3 equiv) in $H_2O$ (1 mL) was added to the reaction mixture, followed by an additional 2 mL $H_2O$ (0.1 M total). Iodomethyl octanoate (0.48 g, 1.7 mmol, 5 equiv) was then added via pipet, followed by an additional 3 mL $CH_2Cl_2$ (0.05 M total). The reaction mixture was stirred vigorously for 40 h and then transferred to a separatory funnel with additional $CH_2Cl_2$ and $H_2O$. The layers were separated, and the organic layer was washed with $H_2O$ (1 × 15 mL). The combined aqueous layers were extracted with $CH_2Cl_2$ (3 × 15 mL). The combined organic layers were washed with brine (1 x 20 mL), dried over $MgSO_4$, filtered, and concentrated *in vacuo* to a brown oil. Purification by column chromatography ($SiO_2$, loaded in toluene, 1.5 to 5% EtOAc in hexanes with 40% $CH_2Cl_2$ as a co-solvent) gave two major products: an orange solid identified as DDAO-7-OME ($R_f$ = 0.71, 10% EtOAc/45% hexanes/45% $CH_2Cl_2$) (0.0239 g, 16% yield) and a yellow-orange solid identified as DDAO-2-OME ($R_f$ = 0.60, 10% EtOAc/45% hexanes/45% $CH_2Cl_2$) (0.0842 g, 63% yield).

**DDAO-2-OME (Figures S15-S18):**

$^1$H-NMR (400 MHz; $CDCl_3$): δ 7.75 (s, 1H), 7.35 (d, *J* = 10.2 Hz, 1H), 6.66 (d, *J* = 1.8 Hz, 1H), 6.66 (dd, *J* = 10.2, 1.8 Hz, 1H), 5.79 (s, 2H), 2.37 (t, *J* = 7.5 Hz, 2H), 1.78 (s, 6H), 1.61 (quintet, *J* = 7.4 Hz, 2H), 1.30-1.24 (m, 8H), 0.86 (t, *J* = 6.9 Hz, 3H).

$^{13}$C-NMR (101 MHz, $CDCl_3$): δ 187.37, 172.87, 153.08, 151.88, 148.31, 141.05, 140.60, 133.40, 132.70, 132.40, 129.64, 128.94, 127.99, 88.14, 38.18, 34.13, 31.74, 29.14, 29.02, 28.93, 24.54, 22.70, 14.19.

ESI-HRMS $[M+H]^+$ m/z calculated for $C_{24}H_{28}Cl_2NO_4$: 464.1390; found: 464.1398.

**DDAO-7-OME (Figures S19-S22):**

$^1$H-NMR (400 MHz; $CDCl_3$): δ 7.62 (s, 1H), 7.62 (d, *J* = 8.7 Hz, 1H), 7.13 (d, *J* = 2.6 Hz, 1H), 7.05 (dd, *J* = 8.7, 2.7 Hz, 1H), 5.84 (s, 2H), 2.38 (t, *J* = 7.5 Hz, 2H), 1.87 (s, 6H), 1.62 (dd, *J* = 14.8, 7.4 Hz, 3H), 1.28-1.22 (m, 10H), 0.84 (t, *J* = 7.0 Hz, 3H).

$^{13}$C-NMR (101 MHz, $CDCl_3$): δ 173.30, 172.62, 159.83, 148.53, 140.59, 140.57, 139.55, 137.12, 136.88, 135.08, 133.98, 114.84, 114.75, 84.48, 39.27, 34.28, 31.72, 29.08, 28.98, 26.86, 24.81, 22.68, 14.18.

ESI-HRMS $[M+H]^+$ m/z calculated for $C_{24}H_{28}Cl_2NO_4$: 464.1390; found: 464.1396.

## Regioisomer determination for the C4 and C8 probes

$^{1}$H-NMR data were used to identify the protons on the methylether unit. We confirmed the identity of the methylether carbon by combining $^{13}$C-NMR with a heteronuclear single quantum correlation (HSQC) experiment. A heteronuclear multiple bond correlation (HMBC) experiment was used to identify the aromatic carbon in the phenolic ether by its relationship to the protons on the methylether, which were three bonds away. Further examination of the HMBC data then allowed us to determine the aromatic proton(s) that were three bonds away from that carbon. The regioisomers were assigned based on whether or not the phenolic ether carbon was correlated with an aromatic proton that exhibited coupling in the $^{1}$H-NMR spectrum. Coupling indicated a regioisomer substituted at the 7-position, whereas no coupling indicated a regioisomer substituted at the 2-position.

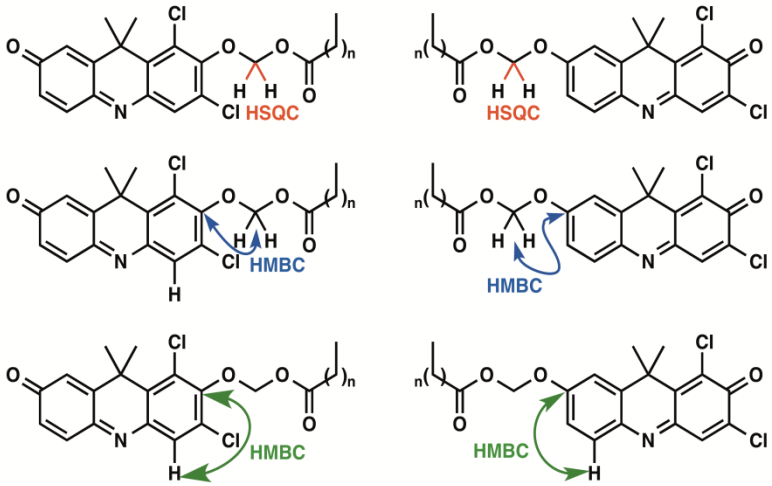


With our data, along with that available from previously reported DDAO-derived compounds,[2–4] we verified a method for determining the regioisomers based on the $^{1}$H-NMR chemical shifts of the protons at the 6 and 8 positions. Substitution at the 2-position is characterized by those protons having a chemical shift between 6.5 and 7 ppm. Substitution at the 7-position is characterized by a chemical shift of 7–7.5 ppm. This assignment strategy was previously proposed by Warther *et al.*, who synthesized the 2 and 7 allyl ether-substituted regioisomers of DDAO and assigned their structures by HSQC and HMBC.[2]


## Spectral characterization of fluorogenic probes

Spectra were acquired on a Tecan Infinite M200 Pro microplate reader in clear 96-well microplates for absorbance reads or black 96-well microplates for fluorescence reads (10 reads per well, 1 nm step size). All measurements were performed in 10 mM HEPES buffer (pH 7.3). In order to remain within the linear range of the instrument, compounds were diluted to 5 µM for absorbance reads and 2.5 µM for fluorescence reads. Compound fluorescence was excited at 602 nm (DDAO), 453 nm (DDAO-7-BME), or 451 nm (DDAO-7-OME). DDAO-2-BME and DDAO-2-OME were nonfluorescent.

The fluorescence of each probe (1 µM) was directly compared to the fluorescence of DDAO (1 µM) by measuring each compound's emission at 670 nm following excitation at 635 nm. The fluorescence decrease, as provided in Table 1, was calculated as the ratio of DDAO fluorescence and fluorogenic probe fluorescence and reported as a fold decrease in fluorescence compared to DDAO.

Extinction coefficients were measured in 10 mM HEPES (pH 7.3). Four independent 5 mM stocks were prepared in DMSO for each compound. Two independent 10 μM solutions were prepared from each stock in 10 mM HEPES (pH 7.3). Absorbance was measured with a Tecan Infinite M200 Pro microplate reader in a Starna Cell 18F-Q-10 quartz cuvette at the wavelength of maximum absorption. The molar extinction coefficients were calculated using Beer's law ($A = \varepsilon cl$; A = absorbance, $\varepsilon$ = extinction coefficient, c = concentration, l = path length). The reported extinction coefficients are the average of eight reads per compound.

The relative quantum yield of DDAO was determined using oxazine 1 (Anaspec, $\phi$ = 0.15 in EtOH) as the reference. The relative quantum yields of DDAO-7-BME and DDAO-7-OME were determined using fluorescein (Sigma-Aldrich, $\phi$ = 0.89 in 0.1 N NaOH) as the reference. A 10 μM solution of each compound was diluted into the appropriate solvent [DDAO, DDAO-7-BME, and DDAO-7-OME: 10 mM HEPES (pH 7.3); oxazine 1: EtOH; fluorescein: 0.1 N NaOH]. The absorbance of each solution was measured on a Tecan Infinite M200 Pro microplate reader in a Starna Cell 18F-Q-10 quartz cuvette. DDAO and oxazine 1 were measured at 520 nm. DDAO-7-BME, DDAO-7-OME, and fluorescein were measured at 400 nm. For each compound, three independent dilutions at a calculated absorbance of 0.01 were prepared from the 10 μM solution. Three samples from each dilution (for a total of $n$ = 9) were excited at 520 nm (DDAO and oxazine 1) or 400 nm (DDAO-7-BME, DDAO-7-OME, and fluorescein) in a 96-well black plate, and the fluorescence emission curves were obtained on a Tecan Infinite M200 Pro microplate reader. The total fluorescence was calculated by integrating the area under the curve using GraphPad Prism 6 software. The quantum yields were calculated as: $\phi_x = (A_s/A_x)\times(F_x/F_s)\times(n_x/n_s)^2\times\phi_s$. In this formula, $\phi$ = quantum yield, A = absorbance, F = total fluorescence, n = refractive index of the solvent, $_s$ = standard, $_x$ = unknown.

**Enzyme panel screen**

Esterases and lipases were purchased from Sigma-Aldrich. Enzymes were prepared as 10 mg/mL stocks and diluted to 1 μg/mL in 10 mM HEPES (pH 7.3). Heat-killed porcine liver esterase (PLE) was prepared by heating PLE at 90 °C for 20 min. The reactions were initiated with 5 μM substrate and incubated for 30 min at 37 °C ($n$ = 4). Probe cleavage was detected by measuring DDAO fluorescence on a Tecan Infinite M200Pro microplate reader ($\lambda_{ex}$ 635 nm, $\lambda_{em}$ 670 nm).

| Esterase | Product # |
|---|---|
| porcine liver esterase | E2884 |
| *Bacillus subtilis* esterase | 96667 |
| *Aspergillus* sp. lipase | 84205 |
| *Candida antarctica* lipase | 65986 |
| *Candida rugosa* lipase | 62316 |
| *Mucor miehei* lipase | 62298 |
| *Pseudomonas cepacia* lipase | 62309 |
| *Pseudomonas fluorescens* lipase | 95608 |
| *Rhizopus arrhizus* lipase | 62305 |

**PLE kinetics**

Probes were evaluated with 50 ng/mL PLE. Kinetic assays were performed in triplicate at 37 °C in 10 mM HEPES buffer (pH 7.3) with 20% (v/v) DMSO as a co-solvent. Probe solutions were pre-incubated at 37 °C for 10 min prior to enzyme addition. After enzyme addition, DDAO fluorescence was measured every 30 s on a Tecan Infinite M200Pro microplate reader ($\lambda_{ex}$ 635 nm, $\lambda_{em}$ 670 nm). Kinetic parameters were calculated using GraphPad Prism 6 software with the method of initial rates.[6] Data were fit to a Michaelis-Menten enzyme kinetics curve, $V = V_{max}[S]/(K_M + [S])$, where $V$ is the reaction rate, S is the substrate concentration, and $K_M$ is the Michaelis constant. Relative fluorescence units were converted to pmol DDAO using a DDAO standard curve.

**PLE detection limit**

PLE (1 pg/mL to 2500 pg/mL) was serially diluted in 10 mM HEPES (pH 7.3) + 20% (v/v) acetonitrile. Reactions were initiated with 25 μM esterase probe and incubated at 37 °C for 10 min ($n$ = 4). Fluorescence was measured on a Tecan Infinite M200Pro microplate reader ($\lambda_{ex}$ 635 nm, $\lambda_{em}$ 670 nm). The detection limit was defined as the lowest statistically significant ($P$ < 0.01) detectable

amount of enzyme compared to the no-enzyme control using an unpaired, two-tailed *t* test with Welch's correction.

### Probe hydrolytic stability

DDAO-7-BME, DDAO-2-BME, DDAO-7-OME, and DDAO-2-OME were diluted to 1 µM in PBS. Samples ($n$ = 6 for each probe) were incubated at 37 °C, and DDAO fluorescence ($\lambda_{ex}$ 635 nm, $\lambda_{em}$ 670 nm) was measured every 10 min for 60 h on a Tecan Infinite M200Pro microplate reader. Since the probes did not completely hydrolyze in PBS within 60 h, each probe was also diluted into PBS containing PLE (10 µg/mL) to determine the fluorescence value of fully-hydrolyzed probe. We used the fluorescence value of PLE-hydrolyzed probe to calculate the percent of each probe hydrolyzed after 60 h (Table S1).

### Fluorescence microscopy of mammalian cells

U2OS epithelial cells were generously provided by Prof. Xiaolin Nan (OHSU). Cells were maintained in Dulbecco's Modified Eagle Medium (DMEM, Gibco®) supplemented with 10% (v/v) FBS (VWR), 100 U/mL penicillin, and 100 µg/mL streptomycin (Invitrogen) in a humidified incubator at 37 °C and 5% $CO_2$. Cells were seeded in an 8-well chambered cover glass (Cellvis) at a density of $5 \times 10^4$ cells per well and allowed to adhere overnight. Cells were counterstained with 1 µg/mL Hoechst 33342 (Invitrogen) before esterase probe treatment. Cells were incubated with 10 µM fluorogenic probe for 10 min at room temperature in Live Cell Imaging Solution (Molecular Probes; 140 mM NaCl, 2.5 mM KCl, 1.8 mM $CaCl_2$, 1 mM $MgCl_2$, 20 mM HEPES). The cells were washed once with additional Live Cell Imaging Solution and imaged in the same medium. Images were collected using a Zeiss 40X/0.95 NA objective on a Yokogawa CSU-X1 spinning disk confocal mounted on a Zeiss Axio Observer microscope at OHSU's Advanced Light Microscopy Core. Hoechst 33342 fluorescence was obtained by excitation at 405 nm (450/50 nm emission filter), and DDAO fluorescence was obtained by excitation at 638 nm (690/50 nm emission filter). Images were processed in ImageJ.[5] The brightness and contrast settings were optimized for the Hoechst nuclear stain, and the same settings were used for all images (Figure S5; false-colored green). Although all six probes produced DDAO fluorescence in live cells (false-colored magenta), the fluorescence varied from probe to probe. Therefore, the maximum brightness and contrast setting was determined separately for each probe. We used the same minimum value for all probes. To enable a direct comparison, the same DDAO settings were applied to a corresponding image of DMSO-treated cells; no far-red fluorescence was detected in DMSO-treated cells using any of our display settings.

### Mycobacterial culture conditions

*M. smegmatis* mc$^2$155 (700084) and *M. marinum* (BAA-535) were obtained from ATCC. *M. bovis* (BCG) was obtained from G. Purdy (OHSU). *Mtb* mc$^2$6020 (Δ*lysA* Δ*panCD* mutant)[7] was obtained from W.R. Jacobs (Albert Einstein College of Medicine, HHMI). These strains were handled as BSL-2 pathogens with appropriate precautions. Cells were thawed from frozen stocks (stored at –80 °C in 6% glycerol). *M. bovis* (BCG), *M. smegmatis*, and *M. marinum* were cultured in 7H9 broth supplemented with 0.5% (v/v) glycerol, 0.05% (v/v) Tween 80, and 10% (v/v) ADC (albumin, dextrose, catalase). *Mtb* mc$^2$6020 was grown in the same 7H9 broth further supplemented with 80 µg/mL lysine, 24 µg/mL pantothenate, and 0.2% (w/v) casamino acids. Cultures were grown at 37 °C (BCG, *M. smegmatis,* and *Mtb* mc$^2$6020) or 30 °C (*M. marinum*) with slow shaking (75–100 RPM).

Wild type *Mtb* CDC1551 (NR-13649) and a CDC1551 transposon mutant for MT2037/Rv1984c (NR-18745) were acquired from BEI Resources and handled as BSL-3 pathogens. Wild type CDC1551 was thawed from a frozen stock, and the transposon mutant was inoculated from an agar slant.

Cultures were grown in 7H9 supplemented with 0.5% (v/v) glycerol, 0.05% (v/v) Tween 80, and 10% (v/v) ADC at 37 °C and 5% $CO_2$ with stirring.

To prepare conditioned medium (CM), *Mtb* mc$^2$6020 was grown to an OD between 0.5 and 1, pelleted, washed twice with Sauton's Minimal Medium, and resuspended in Sauton's Minimal Medium. Cultures were grown at 37 °C with slow shaking (75 RPM). Cells were grown to an OD ~1 and pelleted. The pellet was stored for subsequent lysis (–30 °C), and the clarified CM was sterile filtered through a 0.2 µM membrane (SteriFlip, Millipore) and stored (–30 °C). Thawed CM was subsequently concentrated with a 10 kDa MWCO filter (Amicon).

**Mycobacterial whole-cell assay**

*Mtb* mc$^2$6020 was cultured to an $OD_{600}$ between 0.5 and 1.0 in rich growth medium and then diluted to an $OD_{600}$ of 0.2 in PBS (pH 7.4) with 0.05% Tween 80. Varying numbers of bacilli (3,000,000 to 0) were incubated with 10 µM fluorogenic probe (DDAO-2-AME, DDAO-7-AME, DDAO-2-BME, DDAO-7-BME, DDAO-2-OME, or DDAO-7-OME) for 30 min at 37 °C ($n$ = 4). Cells were treated with phosphate-buffered formalin before DDAO fluorescence was measured on a Tecan Infinite M200Pro microplate reader ($\lambda_{ex}$ 635 nm, $\lambda_{em}$ 670 nm). We determined the significance ($P < 0.05$) of the fluorescence signal produced by each sample compared to a cell-free control using an unpaired, two-tailed $t$ test with Welch's correction. The number of bacilli in each dilution was estimated by assuming that a culture with an $OD_{600}$ of 1 contains $3 \times 10^8$ colony forming units (CFUs)/mL.[8]

**RAW macrophage infection**

RAW 264.7 macrophages were purchased from ATCC and maintained at 37 °C, 5% $CO_2$ in a humidified incubator. Cells were cultured in DMEM supplemented with 10% (v/v) FBS (HyClone™), 100 U/mL penicillin, and 100 µg/mL streptomycin. Near-confluent cells were dislodged with a cell scraper for sub-culturing.

Macrophages ($4 \times 10^7$ cells/flask) in DMEM-FBS (no antibiotics) were infected with *Mtb* mc$^2$6020 ($8 \times 10^8$ bacteria/flask; multiplicity of infection = 20). For mock infection, the same volume of vehicle (DPBS) was added. After a 4 h infection, the cells were washed twice with warm DPBS, and an initial time point was immediately harvested. The remaining flasks were changed to DMEM-FBS with 25 µg/mL amikacin. After 1 h, cells were washed twice with warm DPBS and placed in DMEM-FBS (no antibiotics). At each time point, cells were harvested by centrifugation (3000 RPM, 4 °C) and resuspended in lysis buffer [50 mM Tris (pH 7.5 at 4 °C), 200 mM NaCl, 0.5 mM $CaCl_2$, 0.5 mM $MgCl_2$, 0.2% (v/v) Triton X-100]. Samples were stored at –30 °C prior to lysis by mechanical disruption. The resulting lysates were sterile-filtered (0.2 µm membrane, PALL) and concentrated (10 kDa MWCO filters, Amicon). Protein concentration was determined by BCA assay (Pierce).

**Native PAGE in-gel activity assay**

Cell pellets were resuspended in lysis buffer [50 mM Tris (pH 7.5 at 4 °C), 200 mM NaCl, 0.5 mM $CaCl_2$, 0.5 mM $MgCl_2$, 0.2% (v/v) Triton X-100] and lysed by mechanical disruption. The resulting lysates were sterile-filtered (0.2 µm membrane, PALL), and protein concentration was determined by BCA assay (Pierce). Lysates were resolved by native polyacrylamide gel electrophoresis (10–20% Tris-HCl Criterion gel, Bio-Rad). For mycobacterial profiling, 1 to 8 µg of total protein was loaded per lane, approximately normalized by band brightness. For the macrophage infection samples, an equal amount of total protein (8 µg) was loaded per lane. Gels were run on ice for 2 h at 200 V in 1X Tris-Glycine buffer (Bio-Rad) prepared in deionized water without methanol. Gels were incubated in 10 mM HEPES (pH 7.3) (for DDAO-7-AME, DDAO-2-AME, DDAO-7-BME, and DDAO-2-BME) or 10 mM HEPES (pH 7.3) + 0.1% (v/v) Triton X-100 (for DDAO-7-OME and DDAO-2-OME) containing 5 µM

probe. After 5–10 min, the gels were imaged on a fluorescence scanner (Typhoon 9410 Variable Mode Imager, GE Healthcare). DDAO was detected using a 633 nm excitation laser with a 670 nm (bp 30) emission filter. The resulting images were analyzed in ImageJ.[5]

**Identification of proteins by mass spectrometry**

Esterase bands were excised from a protein gel based on DDAO fluorescence. Gel slices were submitted for protein tryptic digestion, peptide extraction, and LC-MS/MS analysis. For the band excised from whole cell lysate, analysis was performed by the OHSU Proteomics Shared Resource on a Thermo Scientific Orbitrap Fusion (NIH grant S10OD012246). This facility has partial support from NIH core grants P30EY010572 and P30CA069533. The resulting MS/MS spectra were analyzed using Sequest (Thermo Fisher Scientific). Sequest was set up to search the UniProt *M. tuberculosis* H37Rv database (8350 entries) assuming tryptic digestion. Sequest was searched with a fragment ion mass tolerance of 1.0 Da and a parent ion tolerance of 1.5 Da. Carbamidomethyl of cysteine was specified in Sequest as a fixed modification. Scaffold (Proteome Software Inc.) was used to validate MS/MS-based peptide and protein identifications. Peptide identifications were accepted if they could be established at greater than 50.0% probability by the Peptide Prophet algorithm[9,10] with Scaffold delta-mass correction. Protein identifications were accepted if they could be established at greater than 95.0% probability and contained at least 2 identified unique peptides (see Table S2 for a list of identified Culp1 peptides). Proteins that contained similar peptides and could not be differentiated based on MS/MS analysis alone were grouped to satisfy the principles of parsimony.

For the CM bands, analysis was performed by the UC Davis Proteomics Core. The resulting MS/MS spectra were searched using X! Tandem (The GPM, thegpm.org; version CYCLONE 2013.02.01.1). X! Tandem was set up to search the uniprotM_20160127_ja6Dre database (8206 entries) assuming tryptic digestion. X! Tandem was searched with a fragment ion mass tolerance of 20 ppm and a parent ion tolerance of 20 ppm. Carbamidomethyl of cysteine was specified in X! Tandem as a fixed modification. Glu->pyro-Glu of the N-terminus, ammonia-loss of the N-terminus, Gln->pyro-Glu of the N-terminus, deamidation of Asp and Glu, oxidation of Met and Trp, dioxidation of Met and Trp, and acetylation of the N-terminus were specified in X! Tandem as variable modifications. Scaffold was used to validate MS/MS-based peptide and protein identifications. Peptide identifications were accepted if they exceeded specific database search engine thresholds. X! Tandem identifications required at least -Log(Expect Scores) scores greater than 1.5. Protein identifications were accepted if they contained at least 2 identified unique peptides. Proteins that contained similar peptides and could not be differentiated based on MS/MS analysis alone were grouped to satisfy the principles of parsimony.

# Supplementary Figures and Tables

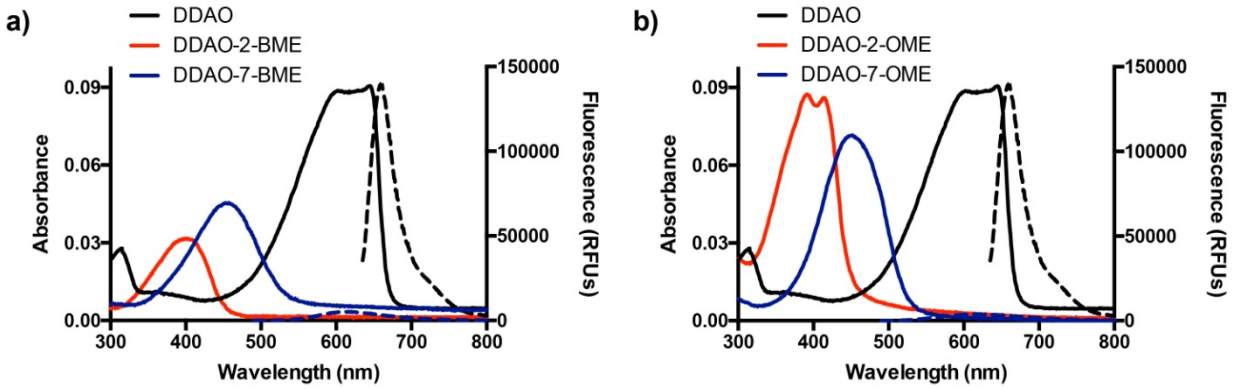


**Figure S1.** The absorbance and emission spectra of DDAO-derived fluorogenic probes. Solid lines indicate absorbance spectra for 5 µM compound and dashed lines indicate fluorescence emission spectra for 2.5 µM compound in HEPES (pH 7.3). a) Spectra of DDAO ($\lambda_{ex}$ = 602 nm), DDAO-2-BME (nonfluorescent), and DDAO-7-BME ($\lambda_{ex}$ = 453). b) Spectra of DDAO ($\lambda_{ex}$ = 602 nm), DDAO-2-OME (nonfluorescent), and DDAO-7-OME ($\lambda_{ex}$ = 451).

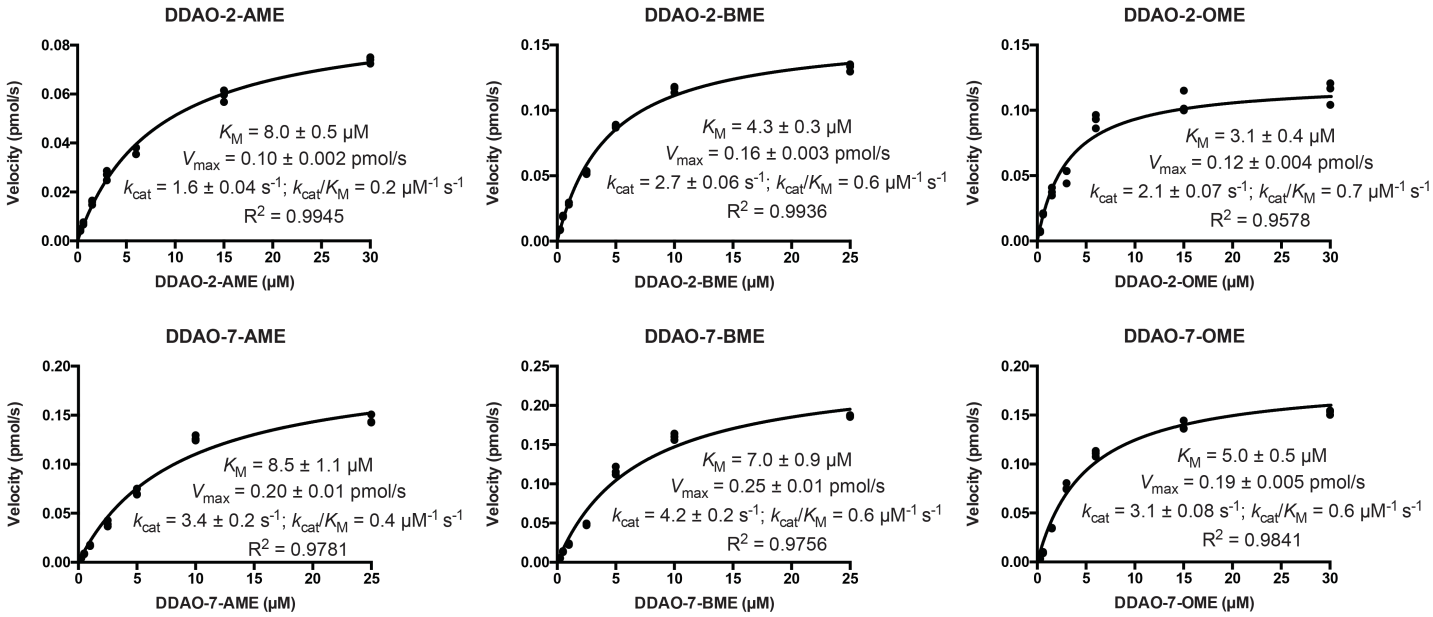


**Figure S2.** Kinetic evaluation of DDAO-derived fluorogenic probes with 500 ng/mL PLE. Reactions were performed in triplicate at 37 °C in 10 mM HEPES (pH 7.3) + 20% DMSO. Probe hydrolysis was detected by measuring DDAO fluorescence ($\lambda_{ex}$ 635 nm, $\lambda_{em}$ 670 nm).

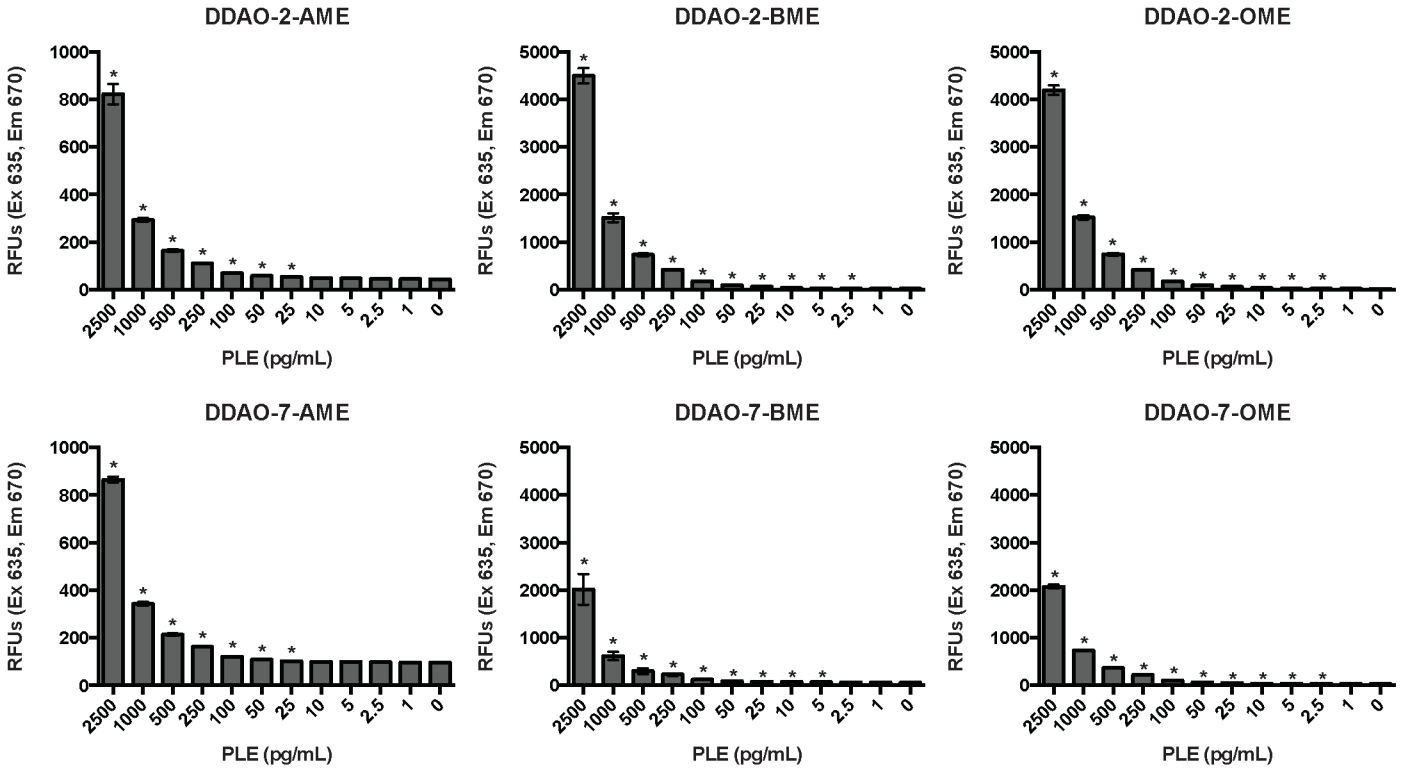


**Figure S3.** Threshold of PLE detection. PLE was diluted in 10 mM HEPES (pH 7.3) + 20% acetonitrile and incubated with 25 µM probe for 10 min at 37 °C. Probe hydrolysis was detected by measuring DDAO fluorescence ($\lambda_{ex}$ 635 nm, $\lambda_{em}$ 670 nm), and the detection limit was determined as the lowest statistically significant signal compared to the enzyme-free control (*$P$ < 0.01). Error bars represent one standard deviation; $n$ = 4.

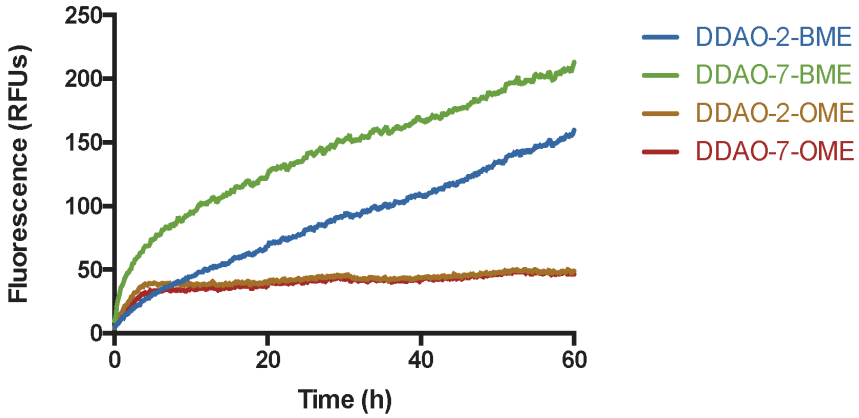


**Figure S4.** The stability of DDAO-derived acyloxymethyl ether probes in PBS (pH 7.4). Probes (1 µM) were incubated at 37 °C, and DDAO fluorescence ($\lambda_{ex}$ 635 nm, $\lambda_{em}$ 670 nm) was measured every 10 min for 60 h ($n$ = 6). Graphs denote the average fluorescence value of all six replicates.

**Table S1. Percentage of DDAO-derived probes hydrolyzed in PBS (pH 7.4) after 60 h.**

| Probe | % Hydrolyzed |
|---|---|
| DDAO-2-BME | 8.0 ± 0.7 |
| DDAO-7-BME | 10.3 ± 0.6 |
| DDAO-2-OME | 2.0 ± 0.1 |
| DDAO-7-OME | 3.4 ± 0.3 |

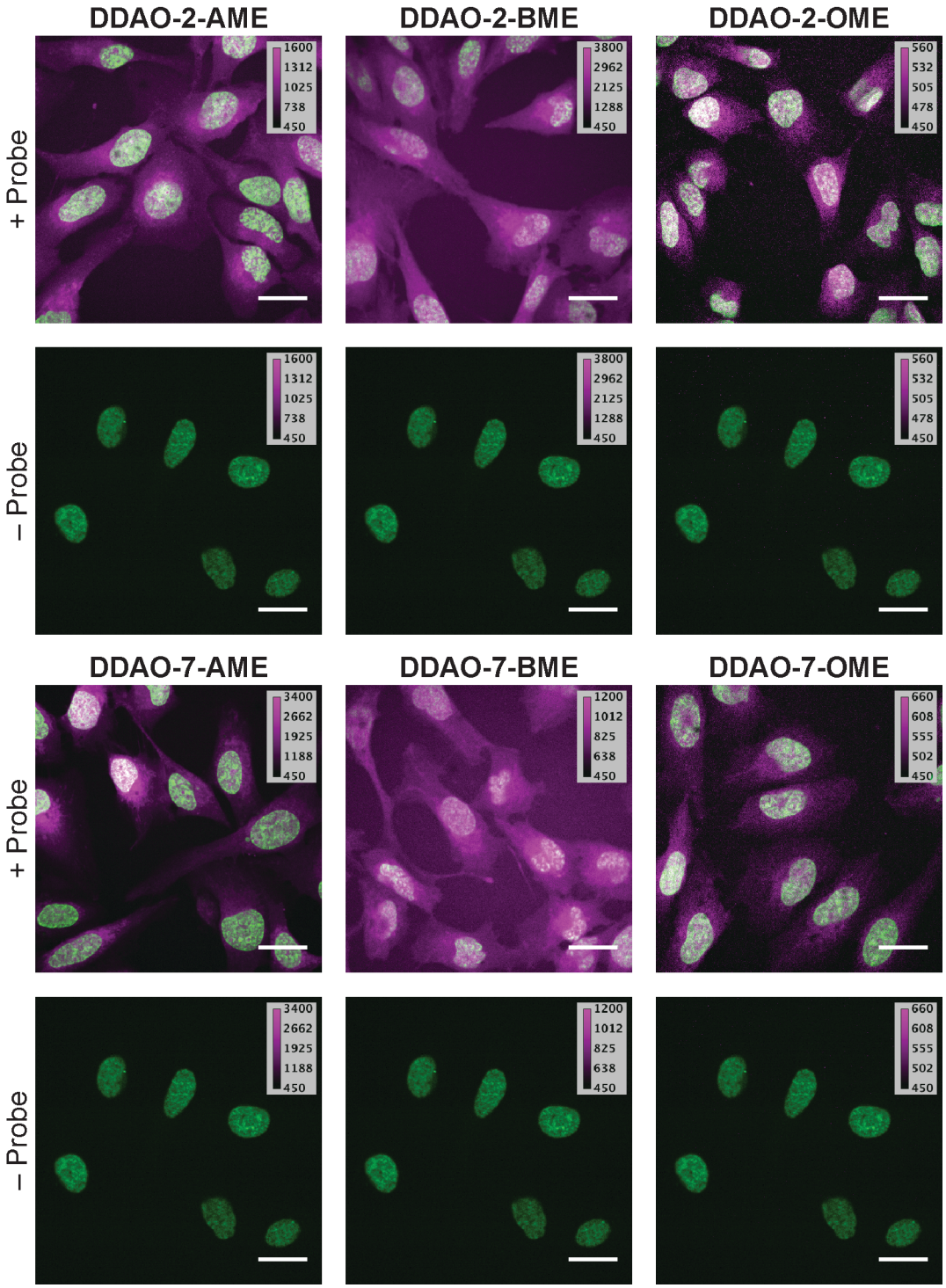


**Figure S5.** Live cell imaging of DDAO fluorescence (magenta) using DDAO-derived fluorogenic esterase probes. Live U2OS cells were counterstained with Hoechst 33342 (green). The maximum DDAO display settings were optimized for each probe, with the minimum and maximum pixel values indicated. A DMSO control (– Probe) is provided to show background fluorescence in the far-red imaging channel, and has been adjusted to match each probe's image settings. Scale bars denote 20 μm.

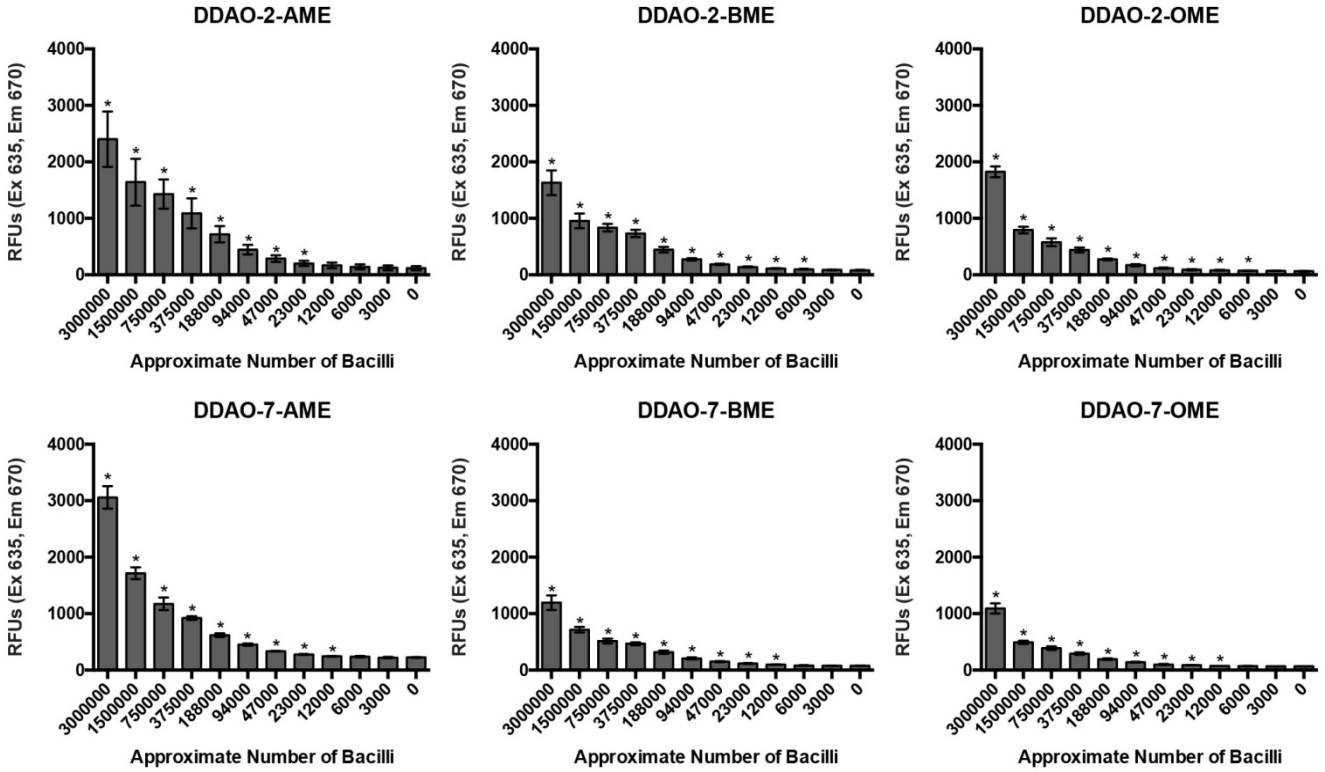


**Figure S6.** Live *Mtb* mc$^2$6020 hydrolyzes fluorogenic probes. Bacilli were incubated with 10 μM probe for 30 min at 37 °C in PBS (pH 7.4) + 0.05% Tween 80. Cells were killed with phosphate buffered formalin before measuring DDAO formation ($\lambda_{ex}$ 635 nm, $\lambda_{em}$ 670 nm). Samples denoted with an asterisk (*) produced statistically significant fluorescence compared to the cell-free control ($P < 0.05$). Error bars represent one standard deviation; $n = 4$.

**Table S2. Identification of Culp1 by mass spectrometry.**

| Sample | Accession | Name | % Coverage | Peptide List[a] | Spectral Counts |
|---|---|---|---|---|---|
| *Mtb* lysate | Rv1984c | Culp1 | 14.7 | R.SIGVYAVNYPASDDYR.A | 3 |
| | | | | R.ASASNGSDDASAHIQR.T | 2 |
| *Mtb* CM (higher band) | Rv1984c | Culp1 | 36.4 | R.ASASNGSDDASAHIQR.T | 14 |
| | | | | Y.AVNYPASDDYR.A | 1 |
| | | | | A.DPCSDIAVVFAR.G | 6 |
| | | | | R.GTHQASGLGDVGEAFVDSLTSQVGGR.S | 6 |
| | | | | R.SIGVYAVNYPASDDYR.A | 5 |
| | | | | R.TVASCPNTR.I | 1 |
| *Mtb* CM (lower band) | Rv1984c | Culp1 | 32.3 | R.ASASNGSDDASAHIQR.T | 3 |
| | | | | A.DPCSDIAVVFAR.G | 5 |
| | | | | R.GTHQASGLGDVGEAFVDSLTSQVGGR.S | 3 |
| | | | | R.SIGVYAVNYPASDDYR.A | 5 |

[a]Periods (.) separate found peptides from the previous and next residues in the protein sequence.

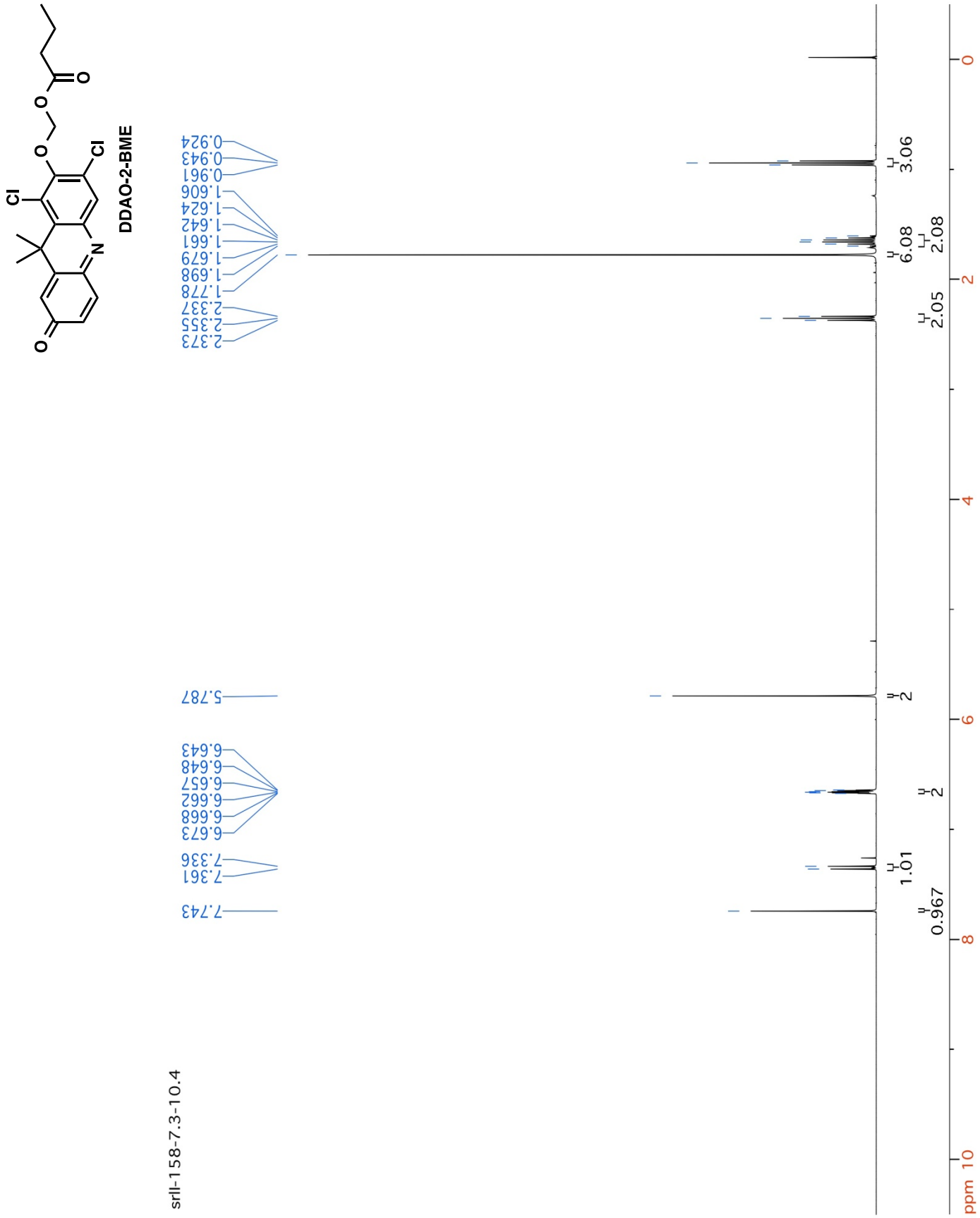


**Figure S7.** $^{1}$H-NMR spectrum of DDAO-2-BME (400 MHz; $CDCl_3$).

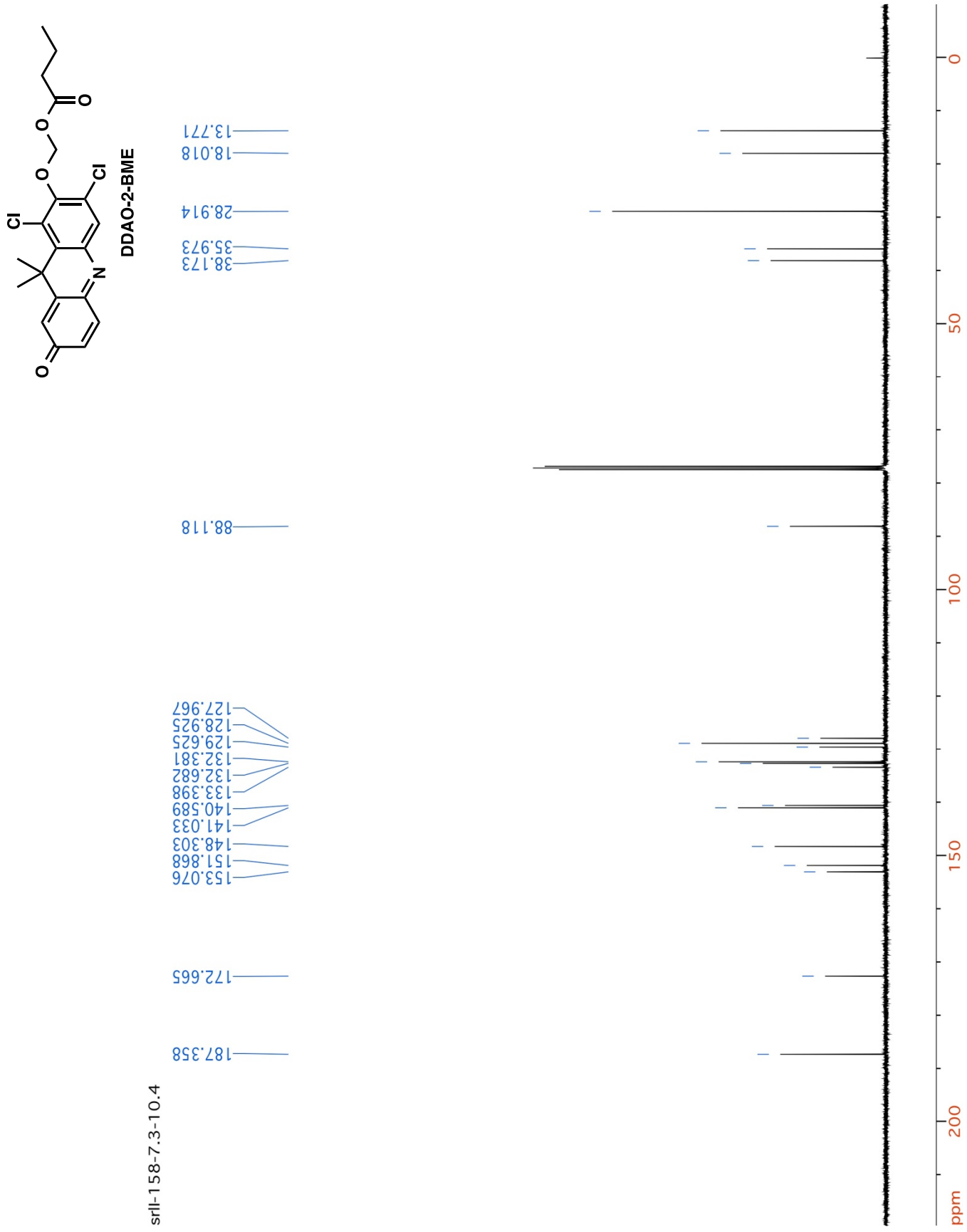


**Figure S8.** $^{13}$C-NMR spectrum of DDAO-2-BME (101 MHz; $CDCl_3$).

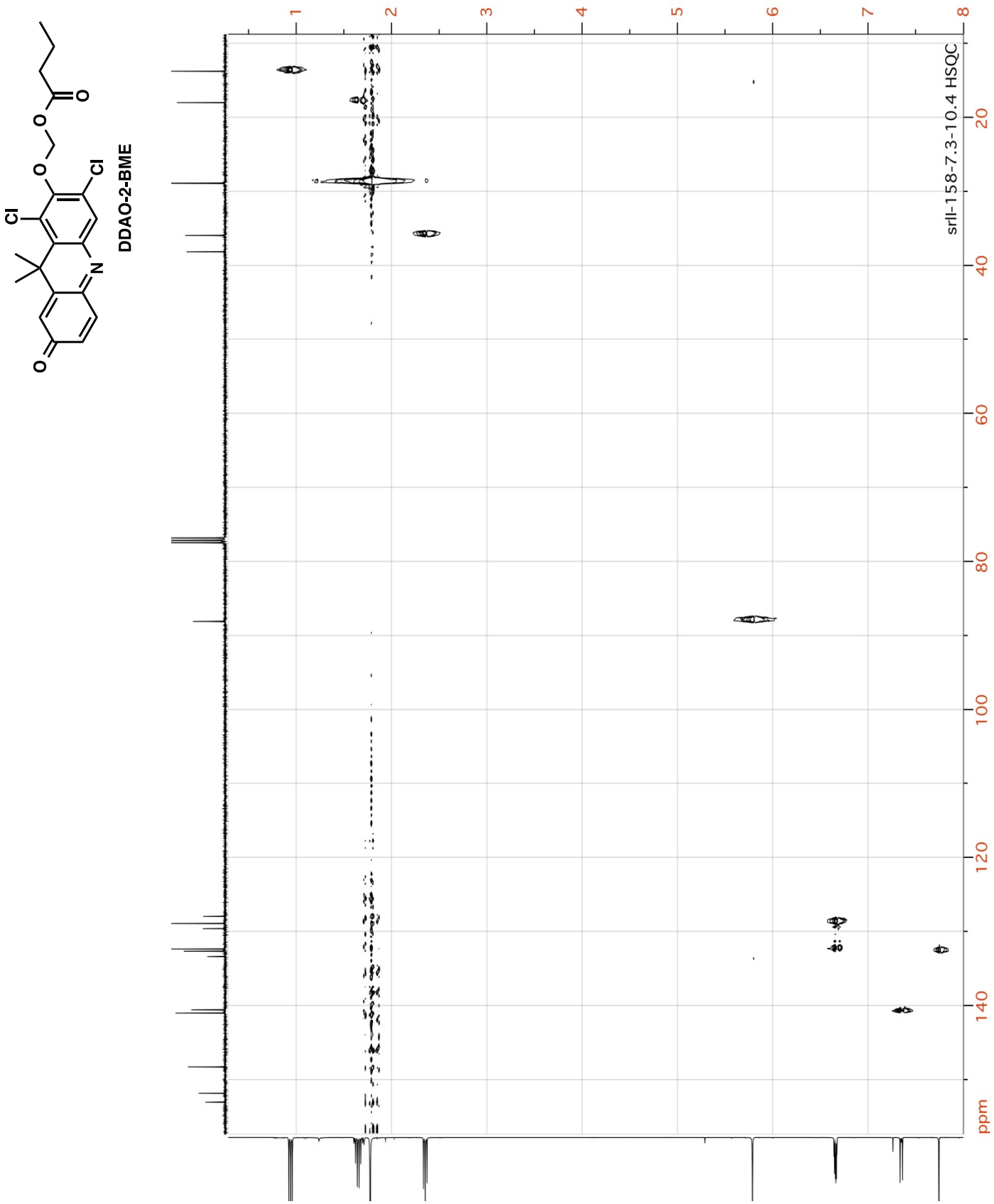


**Figure S9.** HSQC spectrum of DDAO-2-BME ($CDCl_3$).

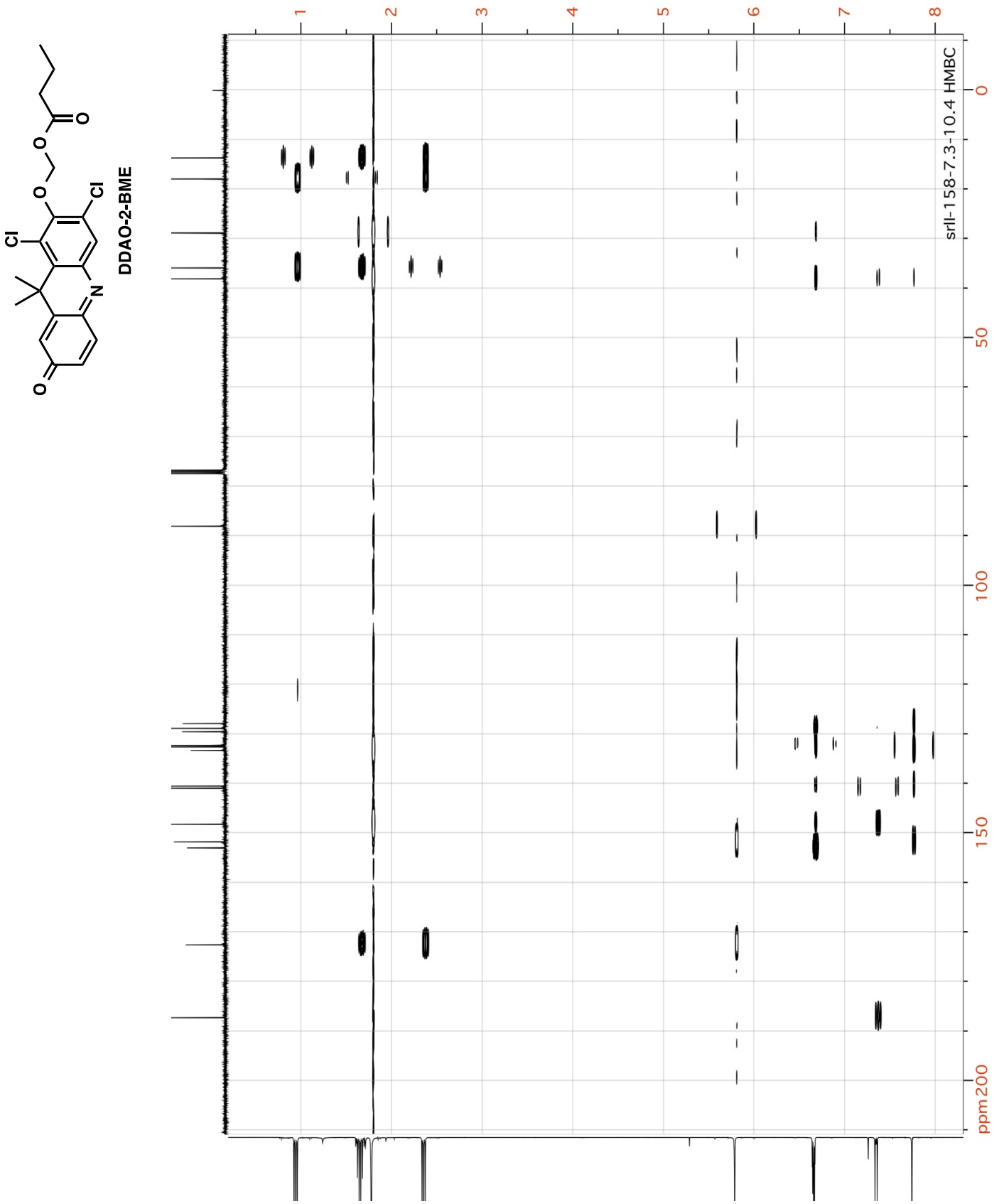


**Figure S10.** HMBC spectrum of DDAO-2-BME ($CDCl_3$).

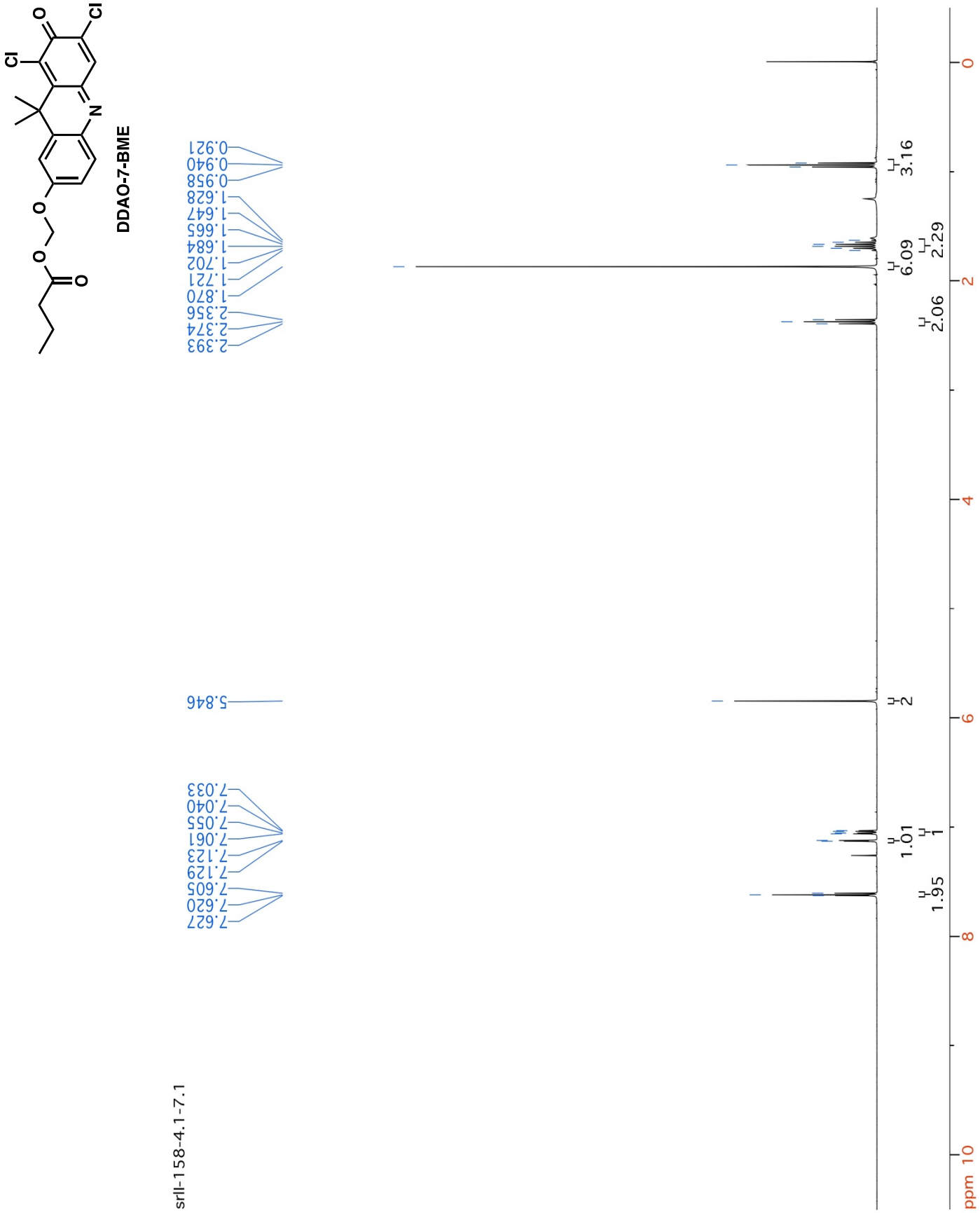


**Figure S11.** $^{1}$H-NMR spectrum of DDAO-7-BME (400 MHz; $CDCl_3$).

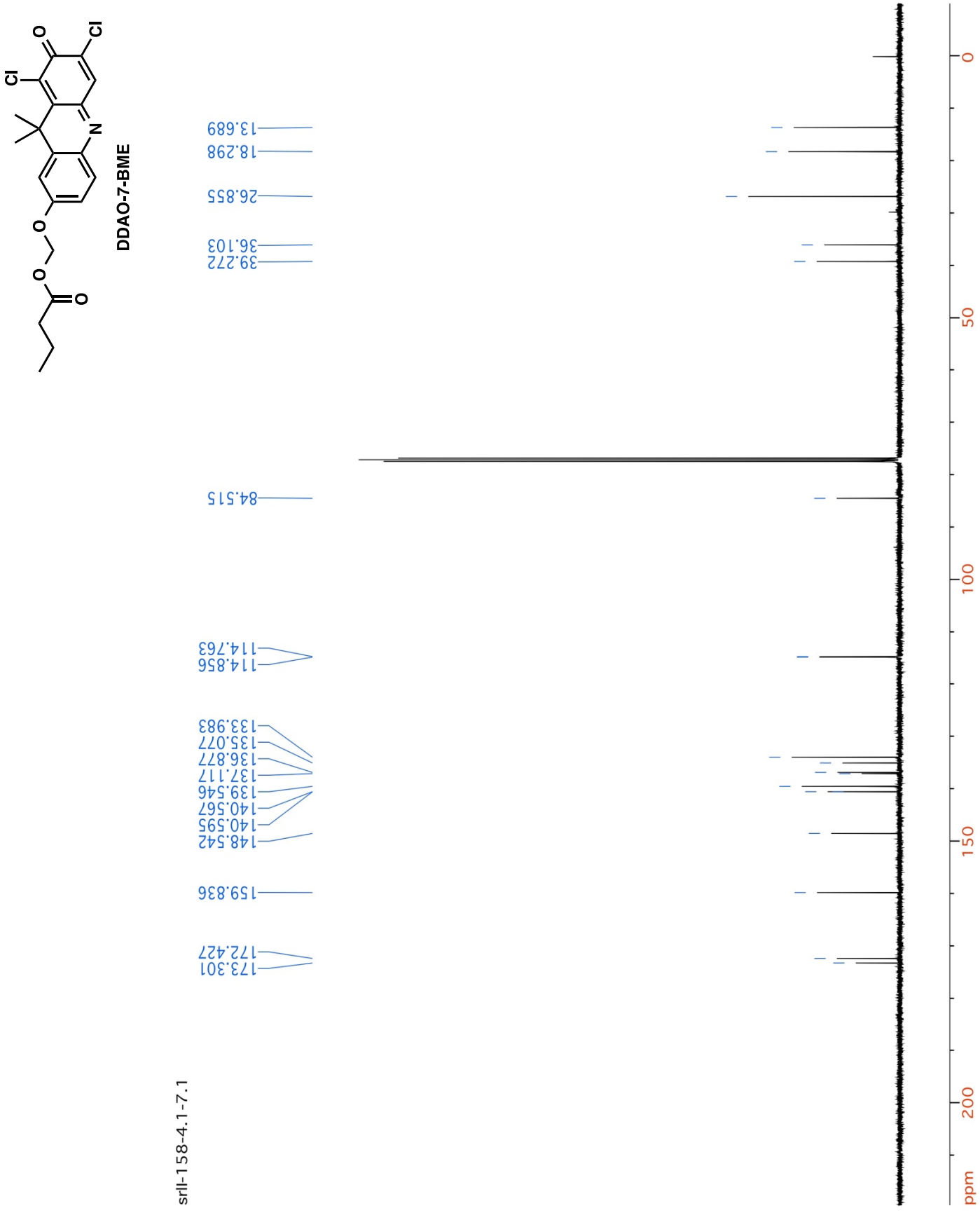


**Figure S12.** $^{13}$C-NMR spectrum of DDAO-7-BME (101 MHz; $CDCl_3$).

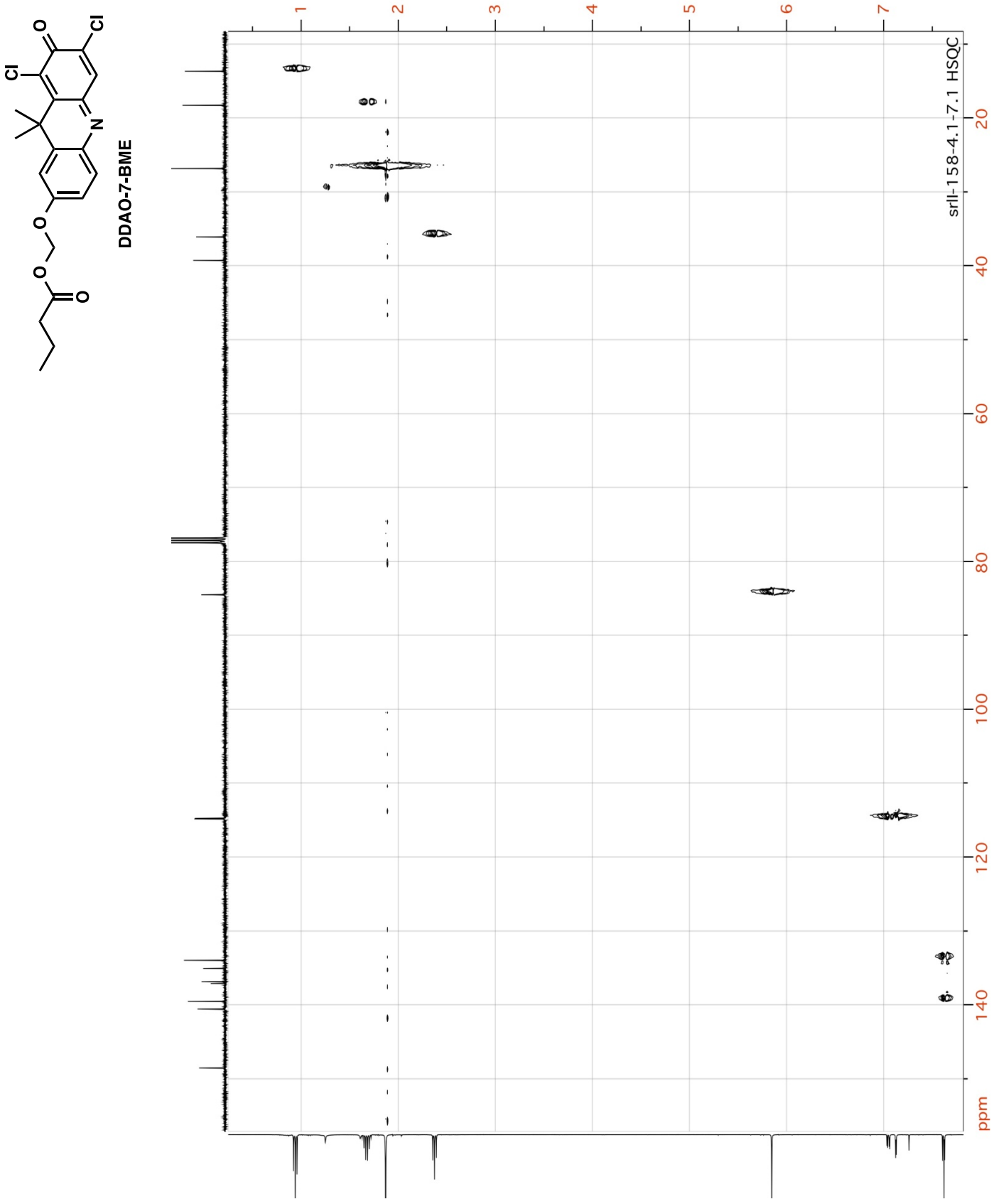


**Figure S13.** HSQC spectrum of DDAO-7-BME ($CDCl_3$).

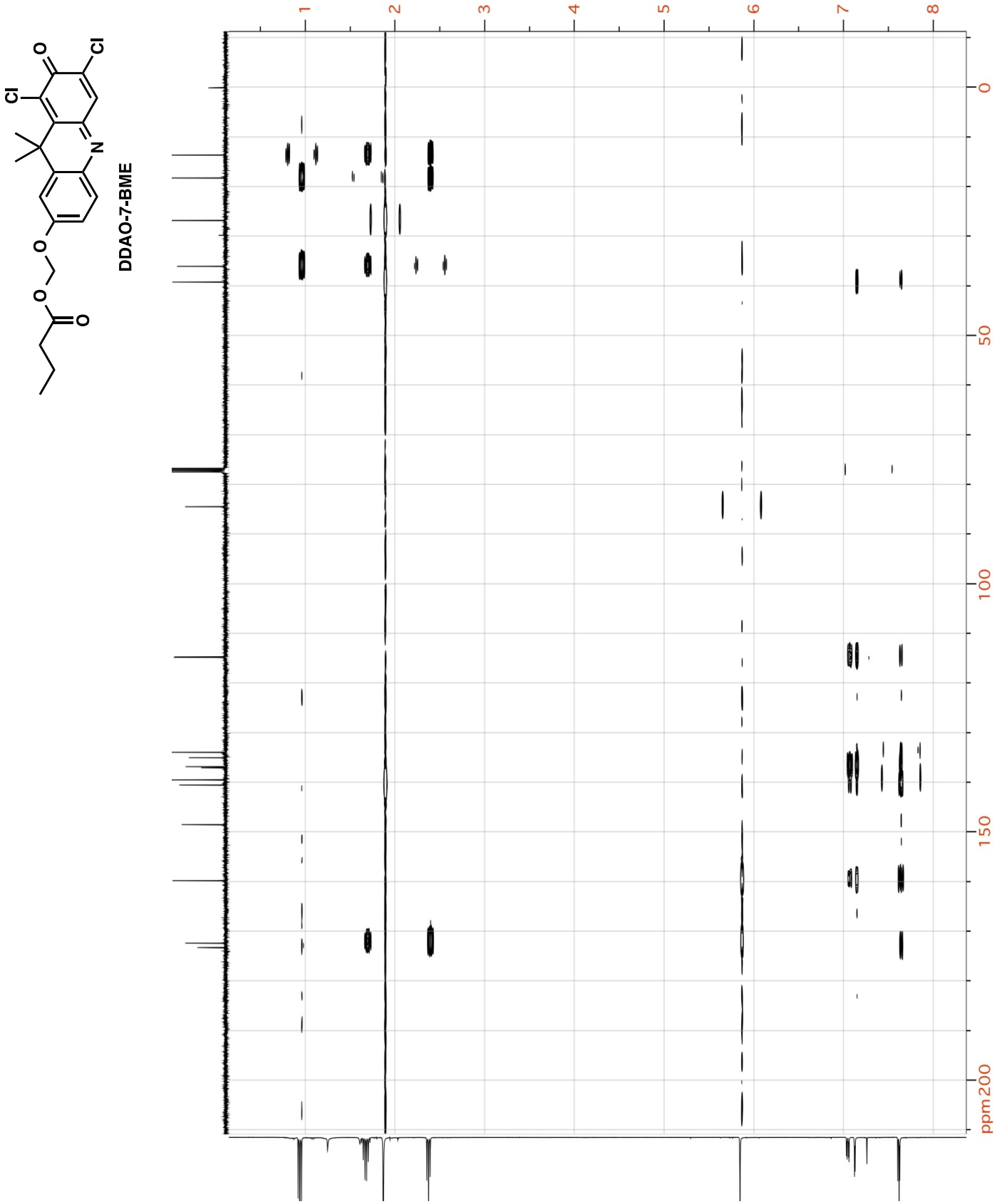


**Figure S14.** HMBC spectrum of DDAO-7-BME ($CDCl_3$).

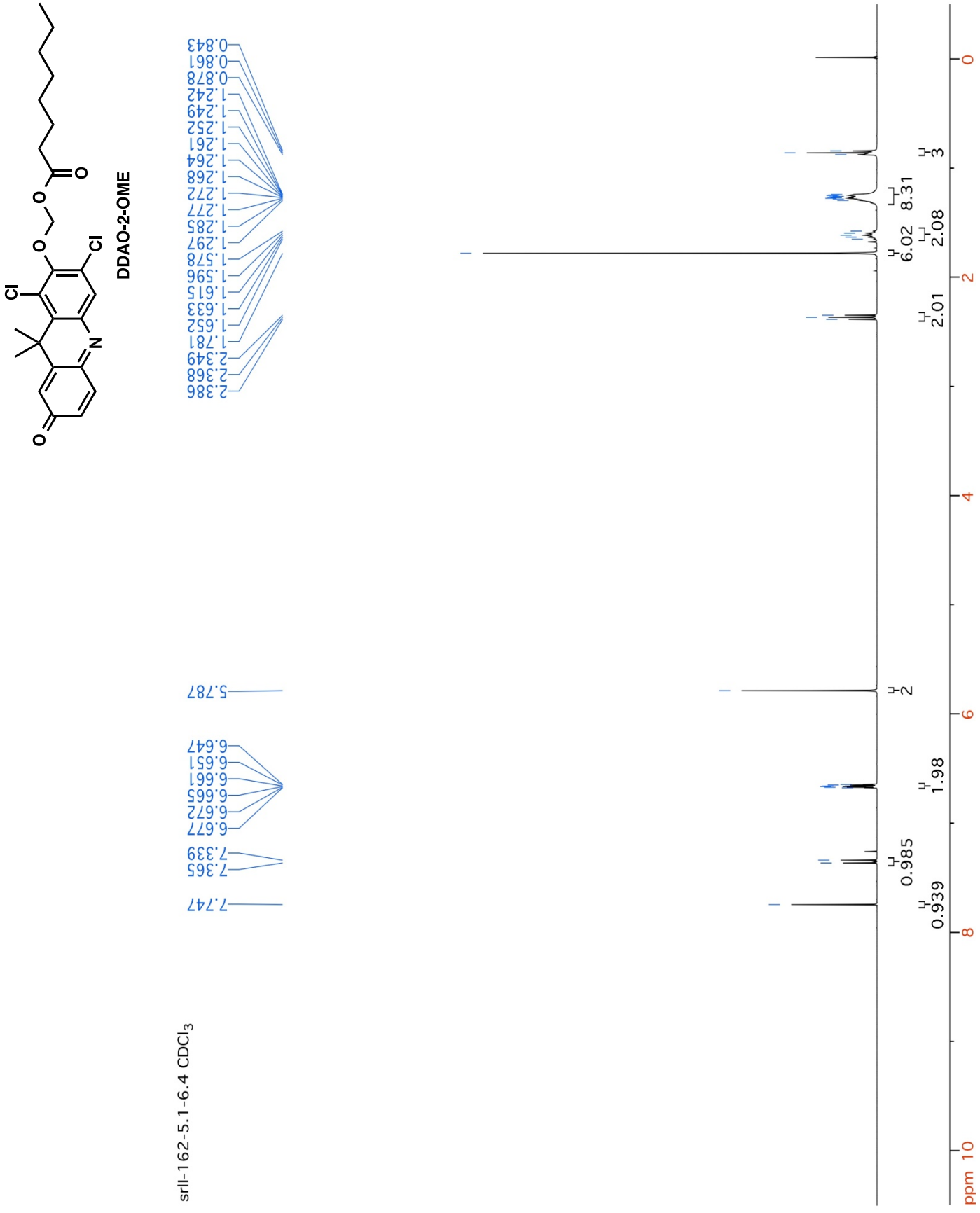


**Figure S15.** $^{1}$H-NMR spectrum of DDAO-2-OME (400 MHz; $CDCl_3$).

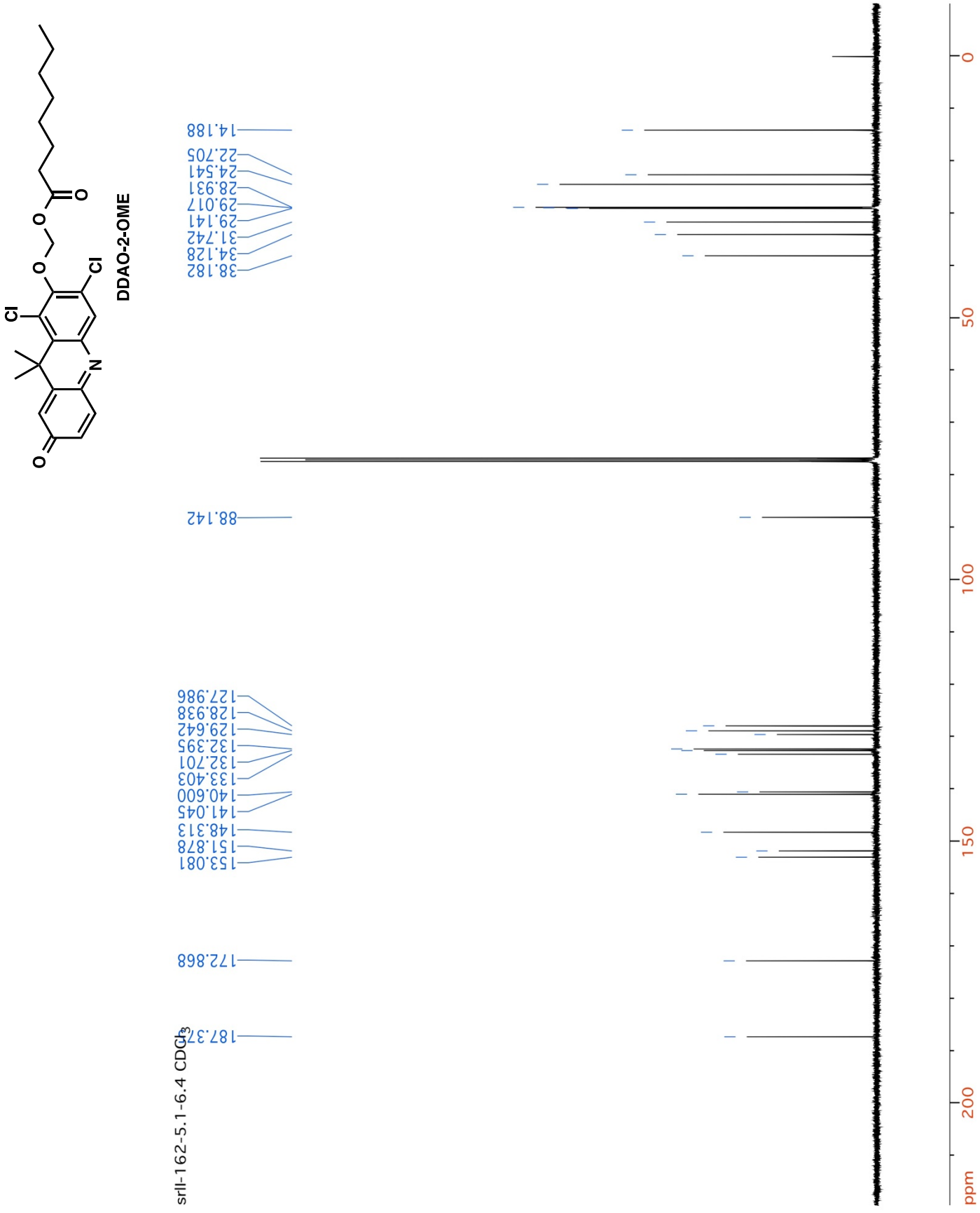


**Figure S16.** $^{13}$C-NMR spectrum of DDAO-2-OME (101 MHz; $CDCl_3$).

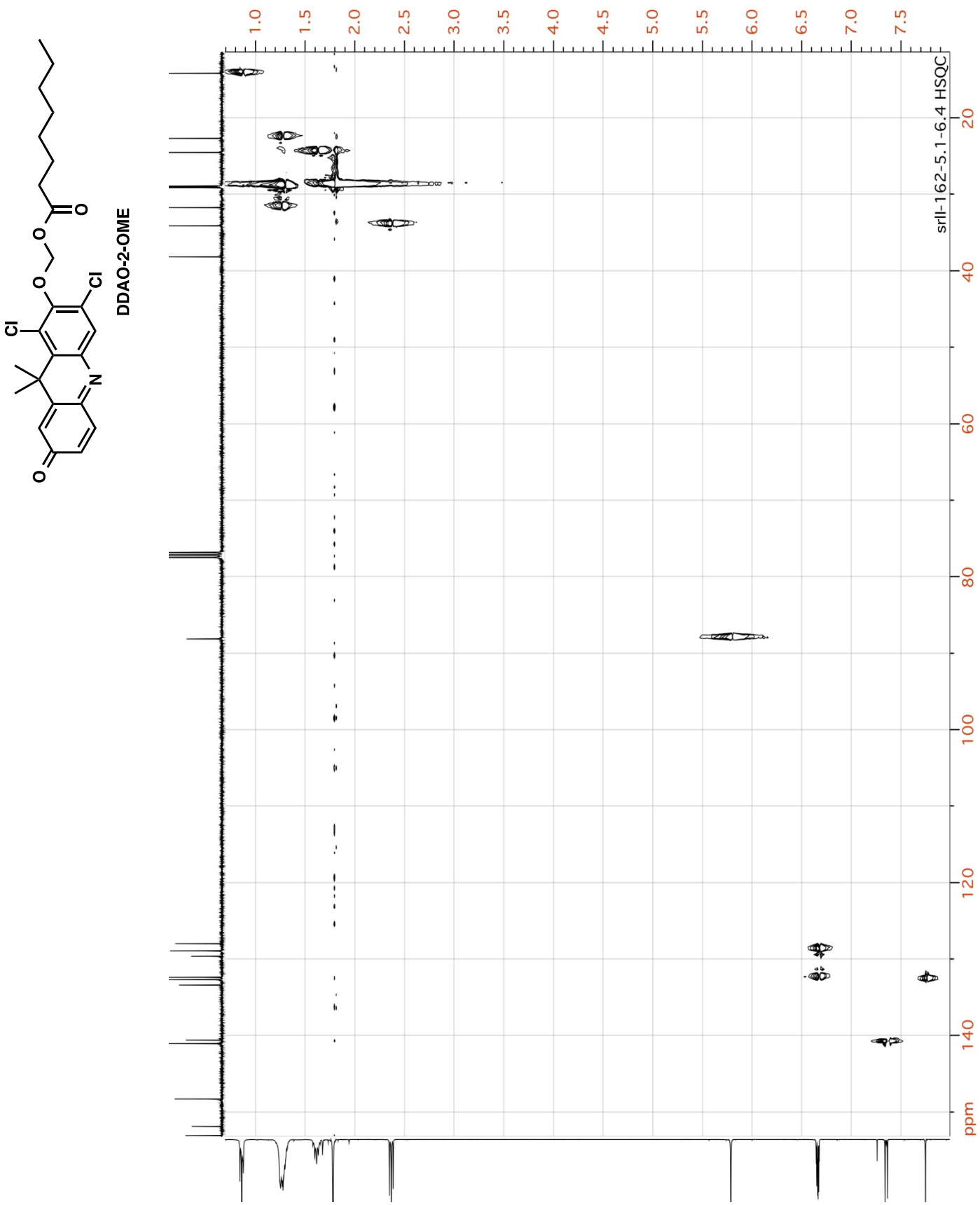


**Figure S17.** HSQC spectrum of DDAO-2-OME ($CDCl_3$).

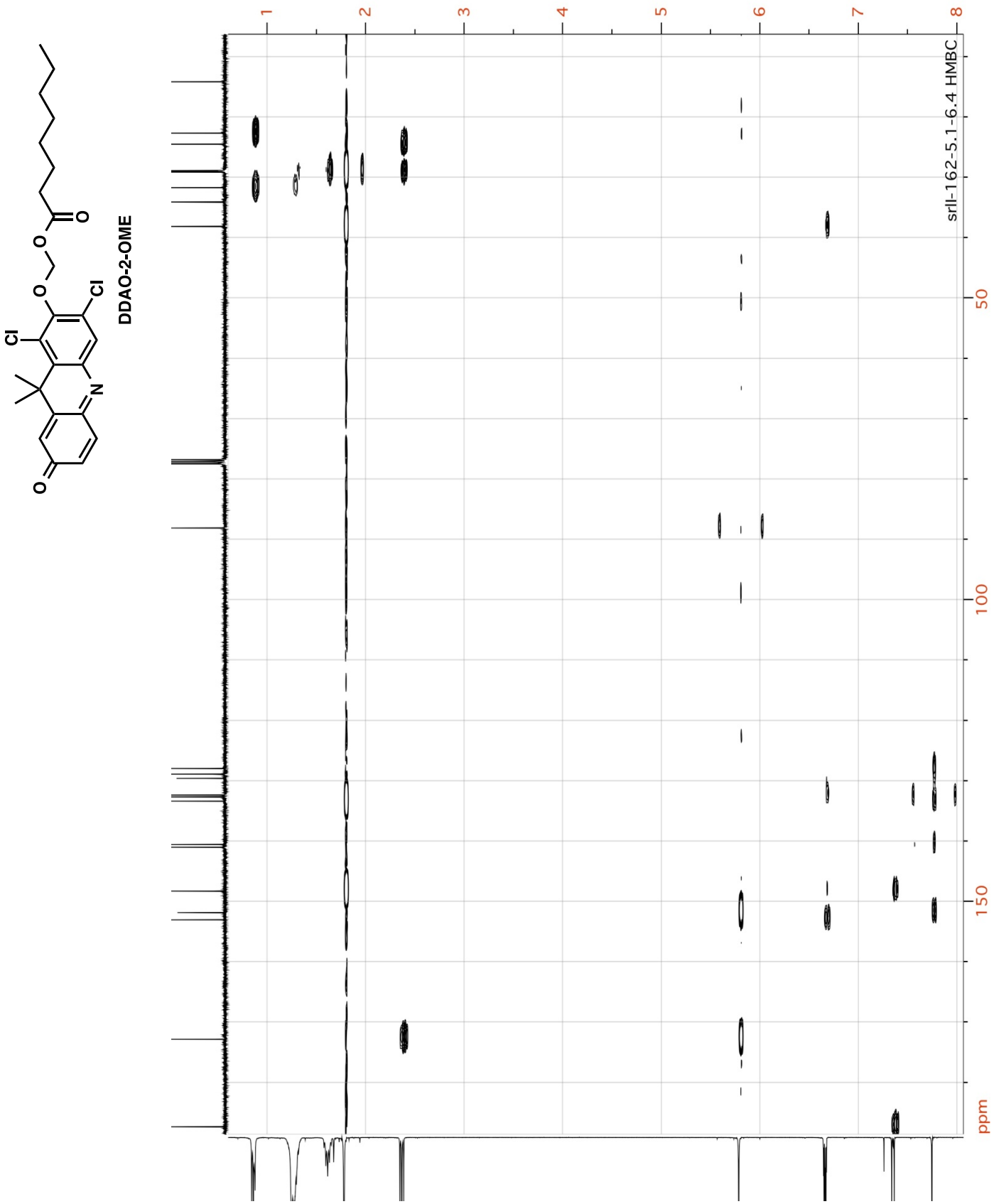


**Figure S18.** HMBC spectrum of DDAO-2-OME ($CDCl_3$).

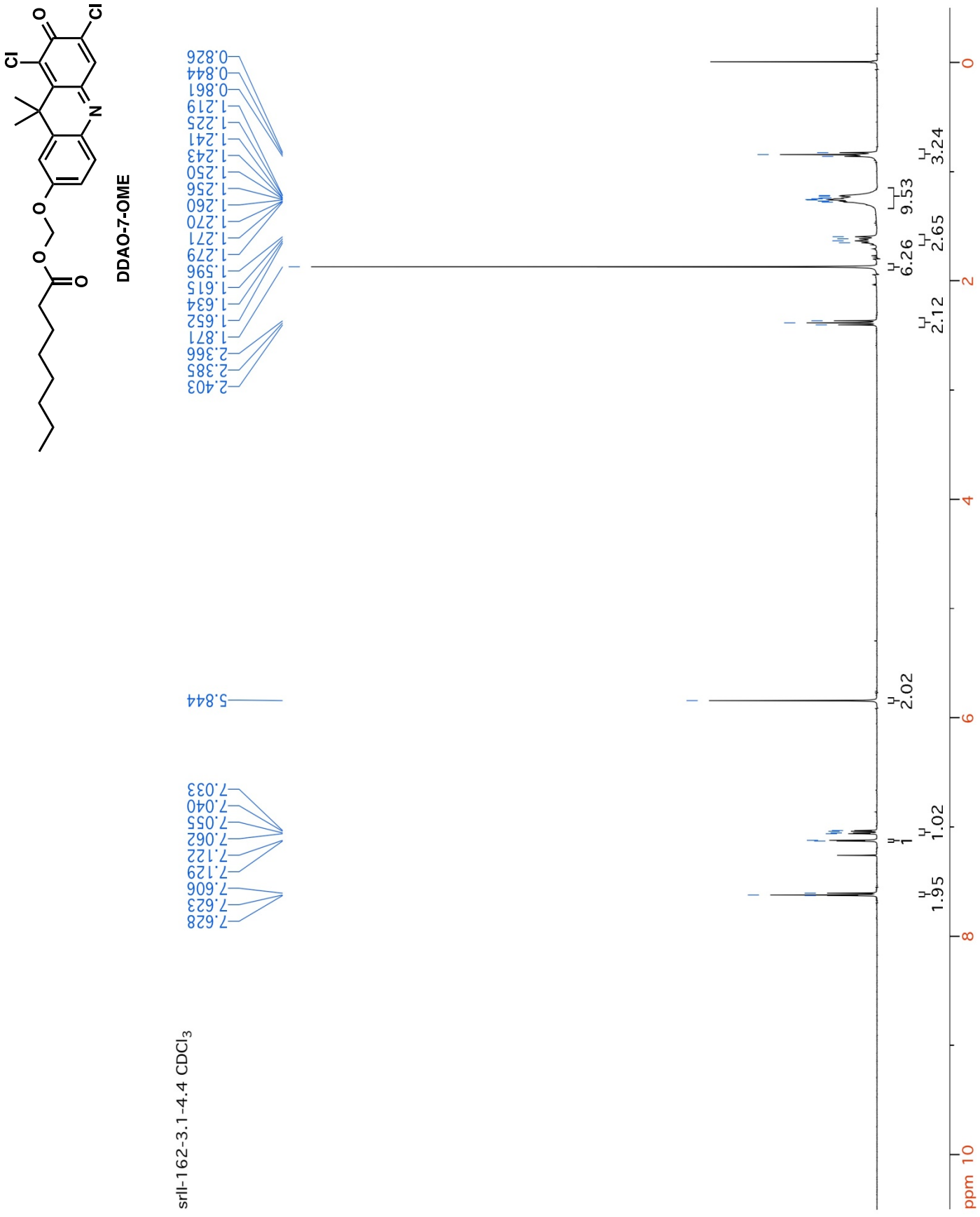


**Figure S19.** $^{1}$H-NMR spectrum of DDAO-7-OME (400 MHz; $CDCl_3$).

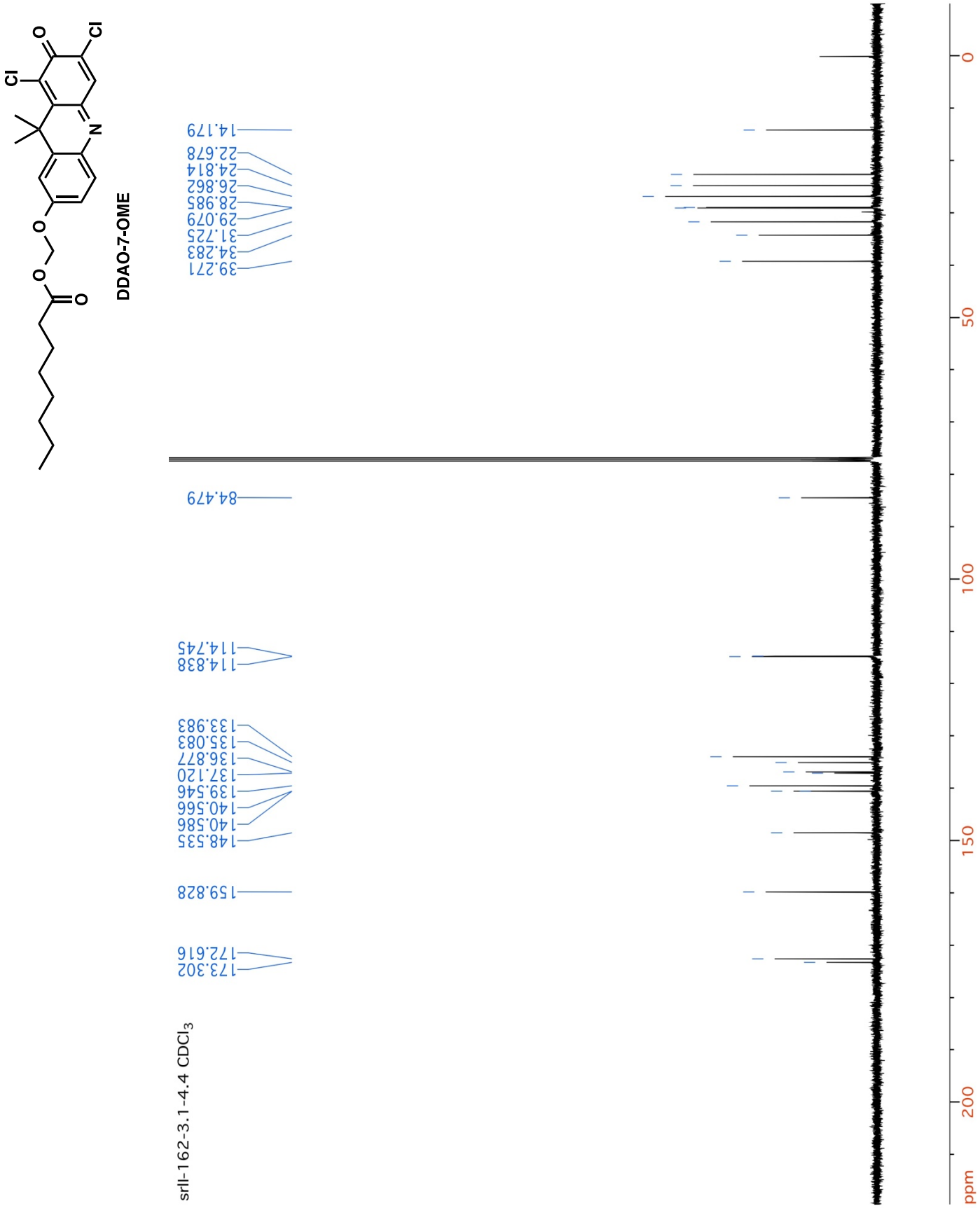


**Figure S20.** $^{13}$C-NMR spectrum of DDAO-7-OME (101 MHz; $CDCl_3$).

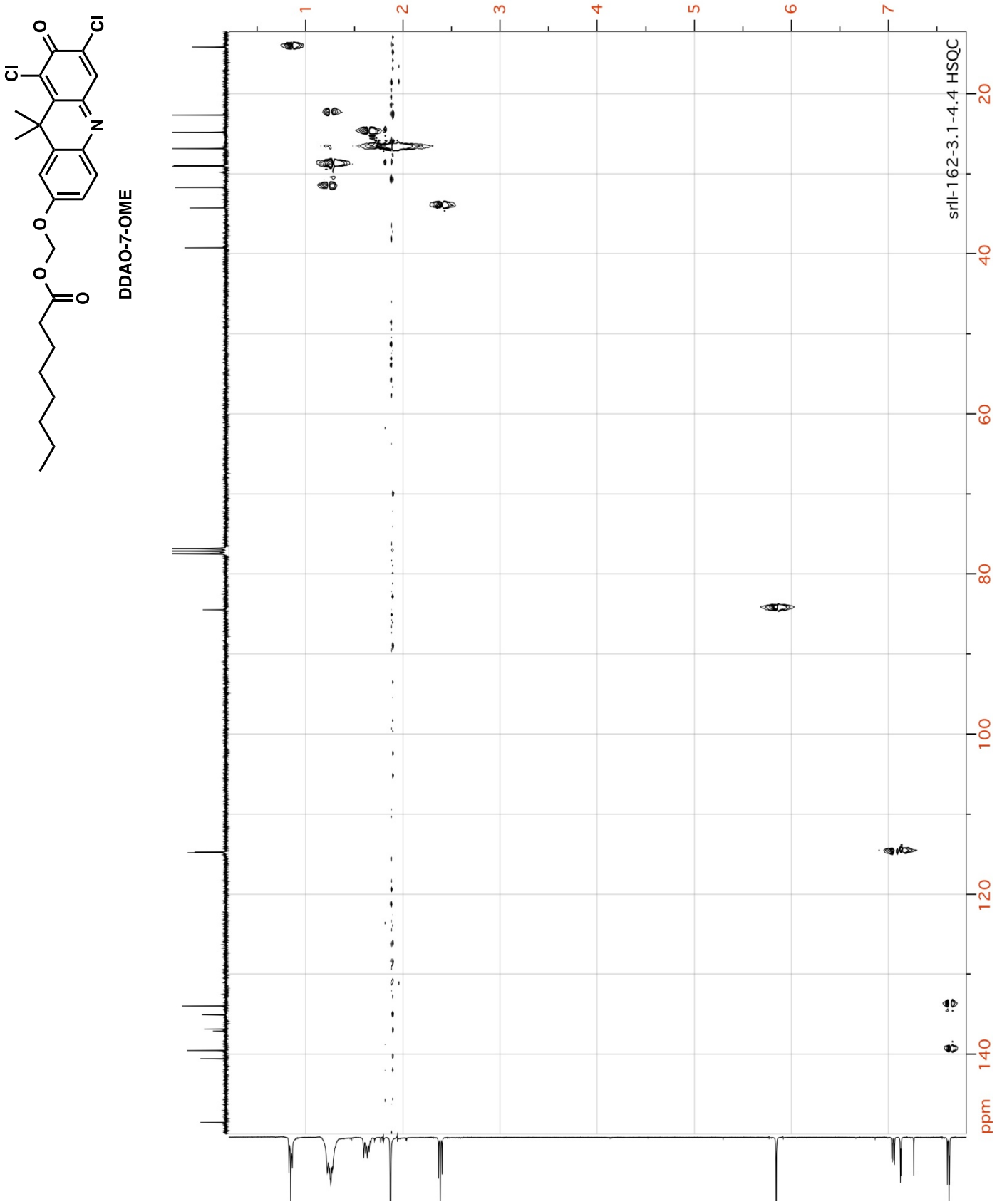


**Figure S21.** HSQC spectrum of DDAO-7-OME ($CDCl_3$).

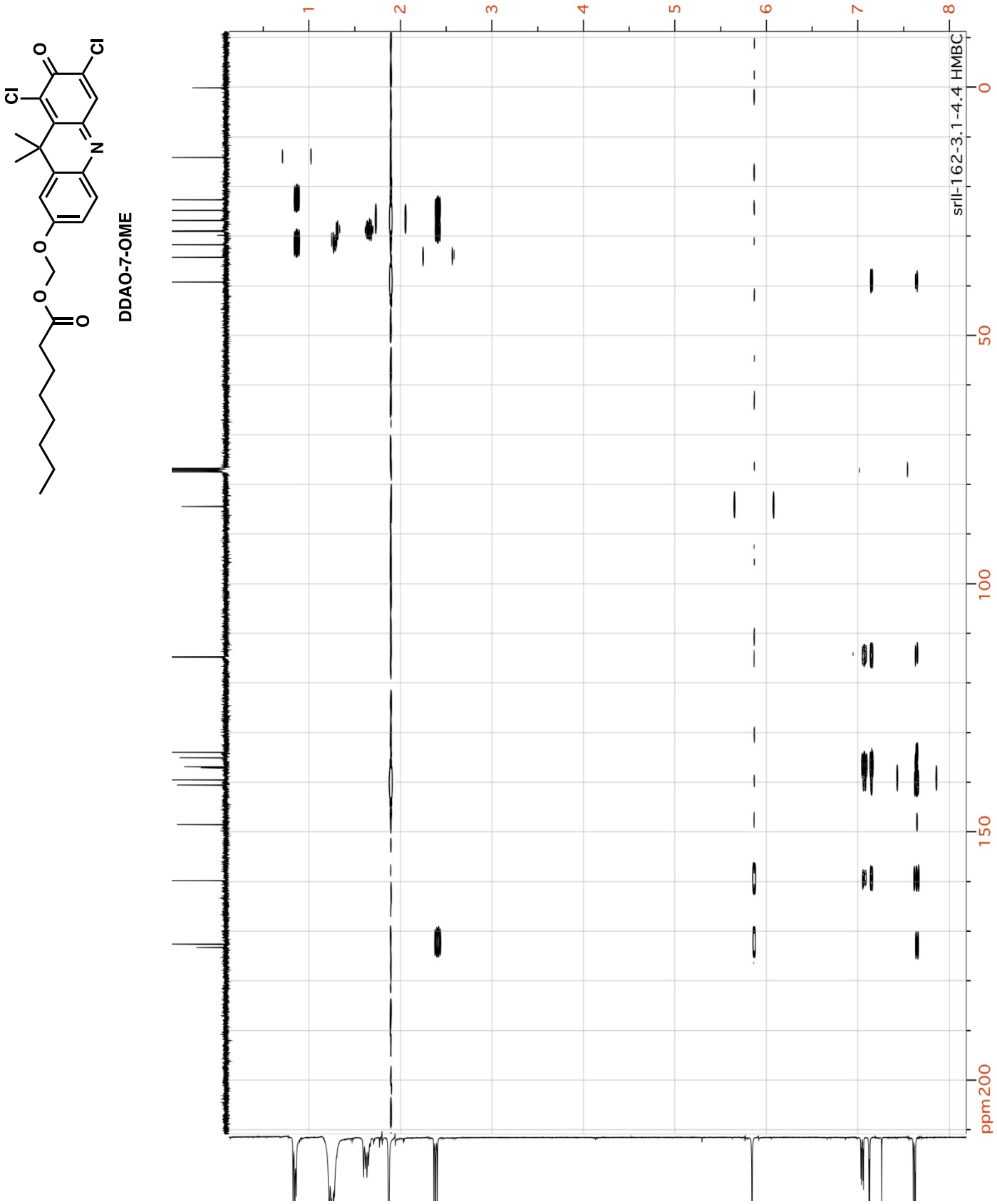


**Figure S22.** HMBC spectrum of DDAO-7-OME ($CDCl_3$).

## References

(1) Azema, J., Guidetti, B., Malet-Martino, M., Martino, R., and Roques, C. (2006) Efficient approach to acyloxymethyl esters of nalidixic acid and in vitro evaluation as intra-ocular prodrugs. *Bioorg. Med. Chem. 14*, 2569-2580.

(2) Warther, D., Bolze, F., Leonard, J., Gug, S., Specht, A., Puliti, D., Sun, X. H., Kessler, P., Lutz, Y., Vonesch, J. L., Winsor, B., Nicoud, J. F., and Goeldner, M. (2010) Live-cell one- and two-photon uncaging of a far-red emitting acridinone fluorophore. *J. Am. Chem. Soc. 132*, 2585-2590.

(3) Duo, T., Goddard-Borger, E. D., and Withers, S. G. (2014) Fluoro-glycosyl acridinones are ultra-sensitive active site titrating agents for retaining beta-glycosidases. *Chem. Commun. (Camb). 50*, 9379-9382.

(4) Tallman, K. R., and Beatty, K. E. (2015) Far-red fluorogenic probes for esterase and lipase detection. *ChemBioChem 16*, 70-75.

(5) Rasband, W. S. (1997-2007) *ImageJ.* U.S. National Institute of Health, Bethesda.

(6) Allison, R. D., and Purich, D. L. (1979) Practical considerations in the design of initial velocity enzyme rate assays. *Methods Enzymol. 63*, 3-22.

(7) Sambandamurthy, V. K., Derrick, S. C., Jalapathy, K. V., Chen, B., Russell, R. G., Morris, S. L., and Jacobs, W. R.,Jr. (2005) Long-term protection against tuberculosis following vaccination with a severely attenuated double lysine and pantothenate auxotroph of mycobacterium tuberculosis. *Infect. Immun. 73*, 1196-1203.

(8) Tufariello, J. M., Jacobs, W. R.,Jr, and Chan, J. (2004) Individual mycobacterium tuberculosis resuscitation-promoting factor homologues are dispensable for growth in vitro and in vivo. *Infect. Immun. 72*, 515-526.

(9) Keller, A., Nesvizhskii, A. I., Kolker, E., and Aebersold, R. (2002) Empirical statistical model to estimate the accuracy of peptide identifications made by MS/MS and database search. *Anal. Chem. 74*, 5383-5392.

(10) Nesvizhskii, A. I., Keller, A., Kolker, E., and Aebersold, R. (2003) A statistical model for identifying proteins by tandem mass spectrometry. *Anal. Chem. 75*, 4646-4658.